TRIBHUVAN UNIVERSITY

INSTITUTE OF ENGINEERING

PULCHOWK CAMPUS

THESIS NO.: PUL079MSGtE019

Numerical Analysis of Geogrid Reinforced Shallow Foundation Overlying Low Plastic Silty Soil

by

Sudeep Neupane

A THESIS

SUBMITTED TO THE DEPARTMENT OF CIVIL ENGINEERING

IN PARTIAL FULFILLMENT OF THE REQUIREMENTS FOR THE

DEGREE OF MASTER OF SCIENCE IN

GEOTECHNICAL ENGINEERING

DEPARTMENT OF CIVIL ENGINEERING

LALITPUR, NEPAL

APRIL, 2026

COPYRIGHT

TRIBHUVAN UNIVERSITY

INSTITUTE OF ENGINEERING

PULCHOWK CAMPUS

DEPARTMENT OF CIVIL ENGINEERING

The thesis titled "Numerical Analysis of Geogrid Reinforced Shallow Foundation Overlying Low plastic silty soil" prepared and submitted by Sudeep Neupane in partial fulfilment of the requirements for the degree of Master of Science (M. Sc.) in Geotechnical Engineering has been examined by us and is accepted for the award of M.Sc. in Geotechnical Engineering by Tribhuvan University.

The undersigned certify that they have read and recommended to Institute of Engineering for acceptance, a thesis entitled "Numerical Analysis of Geogrid Reinforced Shallow Foundation Overlying Low plastic silty soil" submitted by Sudeep Neupane (PUL/079MSGtE/019) in partial fulfillment of the requirement for degree of Master of Science in Geotechnical Engineering.

Supervisor

Prof. Dr. Indra Prasad Acharya

Institute of Engineering,

Pulchowk Campus

External Examiner

Dr. Mohan Prasad Acharya

Senior Geotechnical Engineer

NEA Engineering Company

Dr. Bhim Kumar Dahal

Program Co-Ordinator

M.Sc. in Geotechnical Engineering

Date: April, 2026

DECLARATION

I hereby declare that this study titled “Numerical Analysis of Geogrid Reinforced Shallow Foundation Overlying Low plastic silty soil’ is based on my original research work. Related works on the topic by other researchers have been duly acknowledged. I owe all the liabilities relating to the accuracy and authenticity of the data and any other information included hereunder.

Sudeep Neupane

Roll number: PUL079/MSGtE/019

MSc in Geotechnical Engineering

Date: April, 2026

ACKNOWLEDGEMENTS

I would like to express my sincere gratitude towards my supervisor, Prof.Dr. Indra Prasad Acharya for his invaluable guidance, constant support and encouragement throughout the project. The suggestions provided helped me to develop the research work to the next level. His expertise and encouragement were essential to this study.

I would wholeheartedly like to thank my external examiner Dr. Mohan Prasad Acharya, for his valuable suggestions and guidance for the thesis work. I am also incredibly grateful to our program coordinator Dr. Bhim Kumar Dahal Sir for managing the environment for the completion of the report. Similarly, I extend my gratitude towards Dr. Santosh Kumar Yadav and entire Geotechnical Engineering Department as well as technical and administrative units of Pulchowk campus, Institute of Engineering, for providing resources and conducive research environment for their pivotal role in expanding my perspectives and enhancing my academic journey.

Lastly, I am sincerely grateful to my family and friends for their unwavering inspiration and valuable support throughout my studies. Additionally, I extend my thanks to all the individuals who directly or indirectly contributed to this endeavor.

Sudeep Neupane

Roll No: PUL/079MSGtE/019

ABSTRACT

This research presents comprehensive numerical investigation of the behavior of geogrid reinforced shallow foundation over low-plastic silty soil. Construction of foundation over such soil possesses several geotechnical challenges. This research addresses the particular issue associated with the design of the foundation due to its low bearing capacity and high compressibility at Teku substation, Kathmandu, Nepal. This study explores the soil reinforcement through partial replacement of low plastic silty soil with sand and incorporating with geogrid reinforcement. The unreinforced soil model prepared using Finite element-based software Plaxis 3D was validated against field plate load test to ensure the accuracy and reliability of the model. The validated model was then used to study the influence of various reinforcement parameters, including the depth of placement of first geogrid layer, the number of geogrid layer, the vertical spacing between layers, the thickness of sand fill, and the relative density of sand fill on bearing capacity and settlement characteristics of the foundation. Finally, the result was presented bearing capacity ratio (BCR) and settlement reduction factor (SRF) to quantify the improvement.

The results of the study indicate soil reinforcement with geogrid reinforced sand on low plastic silty soil substantially increases bearing capacity and reduces settlement. The placement of first geogrid layer closer to the footing increases the bearing capacity and reduces settlement. The optimum depth of placement of the first geogrid layer and vertical spacing between reinforcement was found to be in range of (0.2B-0.3B). It was observed that effectiveness of reinforcement is governed by its position within stress influence zone rather than number of reinforcement layer. The depth of sand fill and relative density are found to be crucial for improving both settlement and bearing capacity of soil. The research finding provides new and practical insight for design and optimization of geogrid reinforced soil foundations.

Keyword: Bearing Capacity Ratio (BCR), Settlement Reduction Factor (SRF), geogrid, Soil Reinforcement, PLAXIS 3D

TABLE OF CONTENTS

LIST OF FIGURES

LIST OF TABLES

ABBREVIATIONS AND ACRONYMS

BCR	Bearing capacity ratio
B	Width of Foundation
2D	Two Dimensional
3D	Three Dimensional
EA	Axial Stiffness
FEM	Finite Element Method
RSF	Reinforced Soil Foundation
R.D	Relative Density of Sand
SPT	Stanadard Penetration Test
SRF	Settlement Reduction Factor
u	Depth of placement of First Geogrid Layer
h	Vertical spacing between two geogrid layers
γ	Unit Weight

1 INTRODUCTION

1.1 Outline of study

The main aim of this thesis is to investigate the behavior of shallow footing on geogrid reinforced sand over a low plastic silty soil. This study attempts to evaluate the performance of shallow foundation on weak silty soil reinforced with geogrid layers. The results are organized to show to effect of geogrid position, configuration and combined sand geogrid configuration. A series of models was developed using Finite element-based software Plaxis 3D considering a large number of relevant parameters.

1.2 Background information

Shallow foundation is part of substructure which primarily transfer the structural loads to the underlying soil strata. It used in civil engineering structures due to their simple design, economic value, and simplicity of construction. Their effectiveness depends largely on the strength and compressibility of the subsoil over which they are constructed.

Most of the places of Kathmandu valley consists of silts and silty clay and possess low to very low bearing capacity(K. C. & Raj Dahal, 2020).The construction of infrastructure on weak or loose soil condition is quite challenging as they are prone to extensive settlement, reduced bearing capacity, and often demands the need of ground improvement or soil reinforcement techniques.

The concept of reinforced soil foundation system in which reinforcement layers (geosynthetic product like geogrid, geotextile or natural reinforcement material) are placed beneath footing which was found to be effective in improving bearing capacity, reducing settlement and modify failure mechanism. Many researchers have performed laboratory and field investigation and have concluded that the use of geogrid in improving overall foundation performance. Among several soil reinforcement techniques geogrid has gained popularity because of its grid like structure which enables mechanical interlocking with soil particles. Geogrid offer higher tensile stiffness, chemical resistance, longer design life compared to natural reinforcement making it suitable for foundation reinforcement(Shukla, 2002) (Badie & Wang, 1984).Experimental investigation on rectangular model footing conducted by (Yetimoglu et al., 1994)demonstrated that BCR(bearing capacity ratio) substantially increases with geogrid reinforcement. Development and evolution of numerical tools has enabled detailed investigation of soil-reinforcement interaction and parameters influencing RSF (reinforced soil

foundation) performance which are difficult and time consuming to achieve experimentally. Although numerous experimental and numerical studies have been conducted on sandy soil limited research and focus have been done on geogrid reinforced silty soil of low plasticity and challenges still remains at obtaining optimum geogrid parameters, effect of fill material, considering both shear failure and settlement criteria.

This thesis addresses a gap by performing a numerical analysis of geogrid-reinforced shallow foundation on low plastic silty soil. The unreinforced foundation model is first validated against field plate load test to ensure reliability and realistic simulation of soil behavior. The validated model is then extended to reinforced cases where geogrid is placed within sand fill above low plastic silty soil. A parametric study is conducted to evaluate BCR at different settlement level and SRF factor under different load. The outcomes provide insight into optimum geogrid configuration with respect to BCR and SRF.

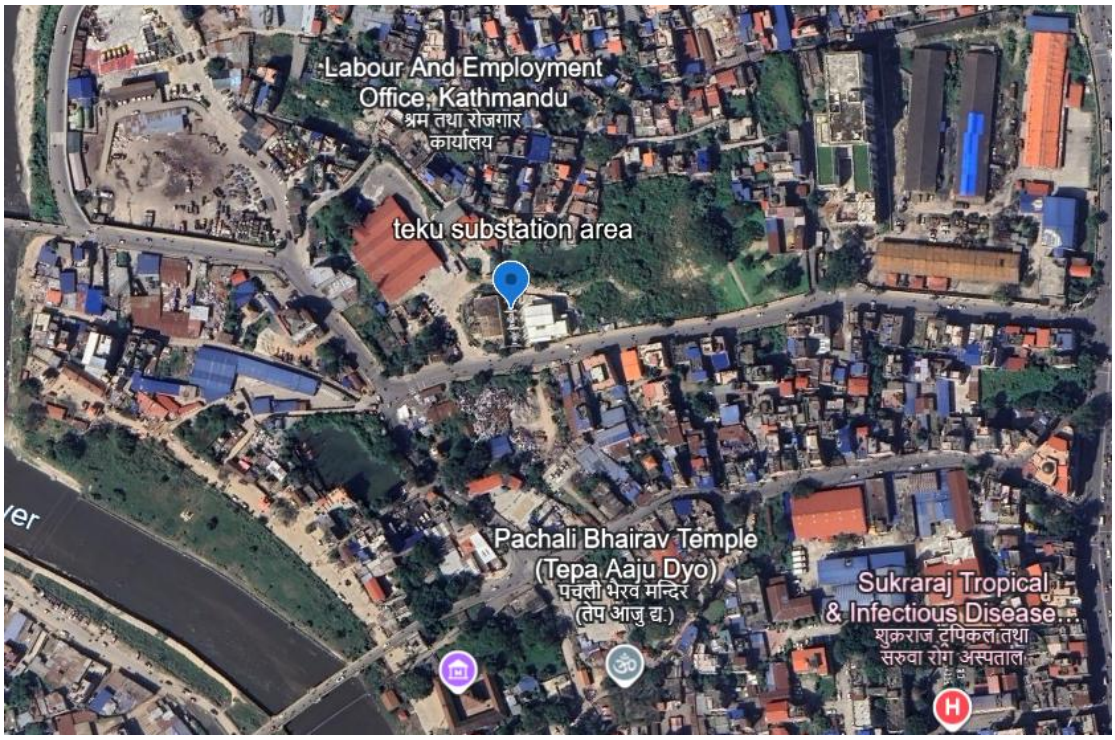

Figure 1.1 Study Area(Teku Substation - Google Earth, n.d.)

1.3 Statement of Problem

Shallow foundation is most common type of foundation used all over the world. Their performance is greatly influenced by strength and compressibility characteristics of supporting soil. For this study soil profile of Teku substation, Kathmandu was considered. As per geotechnical investigation report gray blackish, low plastic silts with fine sand with SPT N value less than 5 usually

prevail up to depth of 15m. Based on SPT N value such soil and can be categorized as weak soil or soft soil. These soils often have Poor strength, high compressibility which makes soil problematic. Construction and design of shallow footings on poor soil strata is quite complex and challenging. A conventional solution for this is to remove and replace the portion of weak soil by granular fill or sand. However, these techniques may sometime require huge thickness of soil replacement which is cost ineffective. An effective solution for this could be partial replacement of weak soil by sand fill with the inclusion of geogrid in between fill. Geogrid has been found be effective for enhancing both bearing capacity and reducing settlement(Sharma et al., 2009). The performance of foundation can be significantly increased by the inclusion of geogrid in between replaced sand. Most of the research have been conducted on the use of geogrid to reinforce sandy and clayey soil, limited research has been conducted on geogrid effectiveness in low plastic silty soil despite of their widespread occurrence. Another challenge stems from the complex geogrid-soil interaction, which cannot be adequately evaluated by laboratory tests only and require numerical analysis. Parameters such as optimum placement of first geogrid, number of reinforcement layers, vertical spacing, and sand cushion thickness all significantly affect footing behavior which has not yet been thoroughly investigated. Numerical modeling, particularly by utilizing finite element procedures (FEM), is a desirable method of simulating such interactions and predicting the behavior of shallow footings with various reinforcement schemes.

This dissertation aims to undertake a comprehensive numerical investigation of the behavior of shallow footings supported by geogrid-reinforced sand over low plastic silty soil. The study focuses on evaluating BCR at different settlement level and SRF at certain load level. The outcomes aim to provide insight into effectiveness of geogrid reinforcement for improving performance of shallow foundation in weak silty soil.

1.4 Objective of study

The major objective of the research is to perform Numerical Analysis of Geogrid Reinforced shallow foundation over low plastic Silty Soil. Some of the other objectives are:

- To construct FE model in plaxis3D to simulate unreinforced plate load test on low plastic silty soil and validate it with field plate load test result to validate the model.

- To extend the validated model to by inclusion of geogrid between sand fill to compare the effect of geogrid and sand reinforcement on bearing capacity and settlement. To conduct parametric study to determine optimum parameter of first embedment depth of geogrid, number of geogrid layers, spacing between geogrid layers, depth of sand fill, effect of relative density of sand fill.
- To evaluate the improvement by measuring bearing capacity ratio (BCR) and settlement reduction factor (SRF).

1.5 Scope of the study

Shallow foundation is usually designed based on shear failure and settlement criteria. So, it is important to evaluate bearing capacity at different settlement levels and settlement at different bearing pressure especially for weak or soft soil condition. The scope of this study is to perform numerical analysis of geogrid reinforced footing and to explore the improvement in performance of foundation in in terms of BCR and SRF.

1.6 Limitation of study

The limitations of the study are:

- Result is case specific and may require calibration for different geogrid types, soil and foundation geometries.
- The sand fill layer was modelled extending across full model width representing an idealized condition.
- Effect of ground water, cyclic loading and consolidation are not considered.
- Geogrid is simulated using built in features in plaxis3D which may not completely represent real geogrid.
- The numerical analysis is performed up to limited settlement level and at specific stress levels.

1.7 Organization of Dissertation

This study is organized into organized into six chapters, heading and subheadings to explain the significant progress made by previous researchers on this field, method used and the main outcomes of this research.

- **Chapter 1** gives a brief introduction to this dissertation. This section presents the problem statement followed by the research objective, scope and limitation.
- **Chapter 2** This section provides overview of literature review on geogrid reinforced foundation, failure mechanism, numerical tools and significant work done by previous researchers on the geogrid reinforced foundation system.
- **Chapter 3** gives a detailed information of overall method and techniques employed to achieve goal and objective of this study. This chapter explains the method of data acquisition, modelling approach and parametric study conducted in this dissertation.
- **Chapter 4** presents the numerical analysis results in systematic and meaningful manner. The results are presented in the form of graph, curves and comparison chart.
- **Chapter 5** This chapter helps to draw conclusions and further recommendation for future work.

2 LITERATURE REVIEW

2.1 Introduction

The use of geosynthetic reinforcement in foundation engineering has gained a lot of attention from both researchers and engineers over the last few decades. With rapid urbanization in developing countries, construction of safe and cost-effective foundations on soft and compressible soil has become a crucial issue. In Nepal, especially in the Kathmandu Valley, is characterized by the presence low-plasticity silty soil. These soils usually have low shear strength, high compressibility, and poor bearing capacity, which creates several problems for shallow foundation design.

To solve these challenges, several ground improvement techniques, such as including deep foundations, soil replacement, and geosynthetic reinforcement have been proposed. Among these, the Reinforced soil foundation system (RSF) has gained a lot of attention due it is cost-effectiveness, simplicity of construction and its effective in improving both bearing capacity and settlement characteristics. In this system, number of reinforcement layer are placed below the foundation or sometime placement of reinforcement layer within a compacted granular fill between the weak soil layer and foundation below. The literature review and significant work done by previous researchers on geogrid reinforced foundation are briefly discussed in this chapter.

2.2 Geogrid

Geogrid are geosynthetic products made of high strength polymer having grid like structures with apertures intersecting each other forming mesh like structure that facilitates interlocking with the surrounding soil. The reinforcing action of geogrid is primarily due to mechanical interlocking of soil particles within their apertures, and due to friction resistance. This property makes geogrid effective for load transfer applications such as slope stabilization, reinforced foundations, road base stabilization and many other geotechnical applications. It is usually manufactured from polypropylene (PP), high density polythene (HDPE), polythene (PTE) materials. The use of geogrid for foundation reinforcement has been effective to reduce settlement, to increase stiffness of soil and to enhance bearing capacity have been established by several researchers and literatures. It can also be classified as extruded, woven and boned on the basis of manufacturing process. Geogrid are basically classified into three main types:

a) Uniaxial geogrid: They are made by stretching of polymer sheets in longitudinal direction due to which it possesses higher tensile strength primarily in one direction (longitudinal) as compared to transverse direction.

b) Biaxial: They are made by stretching of polymer sheets in both longitudinal and transverse direction. These geogrids are equally strong in both longitudinal and transverse direction.

c) Triaxial: Possess It usually are made in triangular or hexagonal pattern, distribute load in multiple direction making it suitable for high stress distribution.

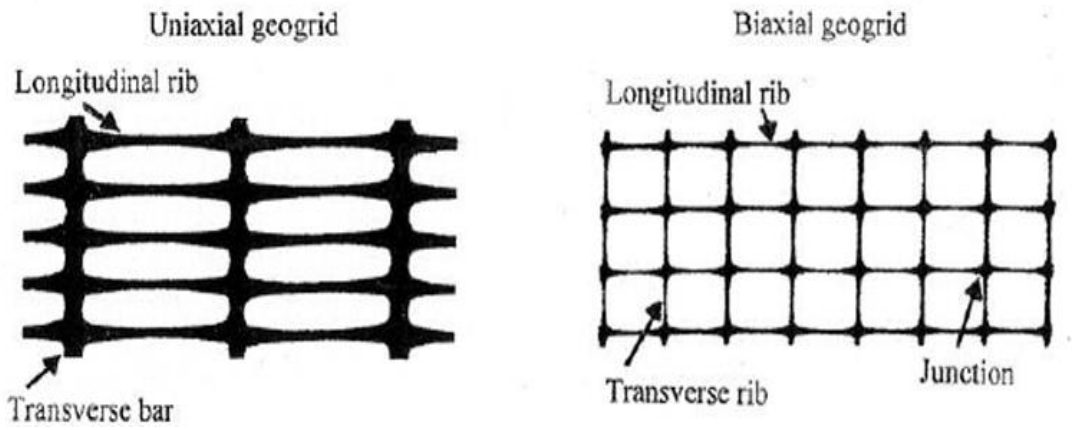

Figure 2.1: Uniaxial and Biaxial geogrid(Das, 2016)

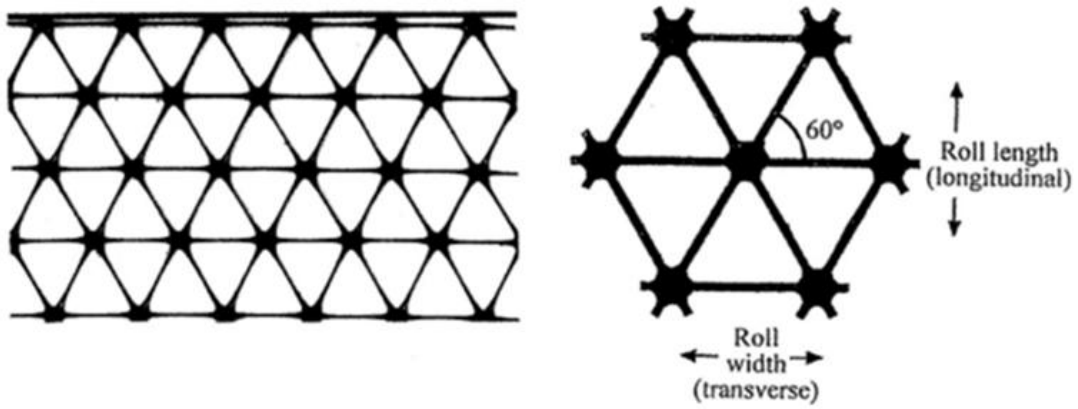

Figure 2.2 Triaxial geogrid(Das, 2016)

2.3 Key properties

The performance of geogrid is greatly dependent on physical and mechanical properties of geogrid. Some of the key properties of geogrid are;

- Tensile strength: It refers to maximum force that geogrid can withstand while being pulled or stretched before it ruptures or fail. It is usually measured in KN/m.
- Stiffness: It is ability to resist deformation or elongation under applied load. It is expressed as ratio of tensile force to corresponding strain.
- Aperture and junction strength: To transfer stress between ribs without failure aperture and junction strength is crucial.
- Aperture size and shape: It is crucial factor as it governs mechanical interlocking, confinement mechanism in geogrid soil interaction.
- Elongation and Flexibility: To incorporate changes in soil and surrounding geogrid require some flexibility and elongability. As too flexible can't hold structure firmly and too rigid can cause crack under pressure. However, balance between tensile strength and elongation is essential for proper functioning of geogrid.

2.4 Concept of Reinforced Soil Foundation

Soil reinforcement is a technique of improving the engineering properties of soil by inclusion of stiffer element. Soil usually has considerable strength in compression strong in compression but weak in tension. When the load is applied soil deforms and it fails when shear stress is less than the shear strength of material. This failure is mainly due to the lack of tensile resistance required to resist lateral spreading induced due to load. Initially metallic bar, rods, plastic sheets, bamboo were arranged in specific pattern for soil reinforcement. concept of soil reinforcement tensile element in soil to improve its strength. With the development and advancement in polymer technology, the use of geogrid, geocell, and geonets has gained popularity nowadays. Geogrid improves soil stiffness, and has a longer design life compared to natural reinforcement, making it suitable for foundation reinforcement.

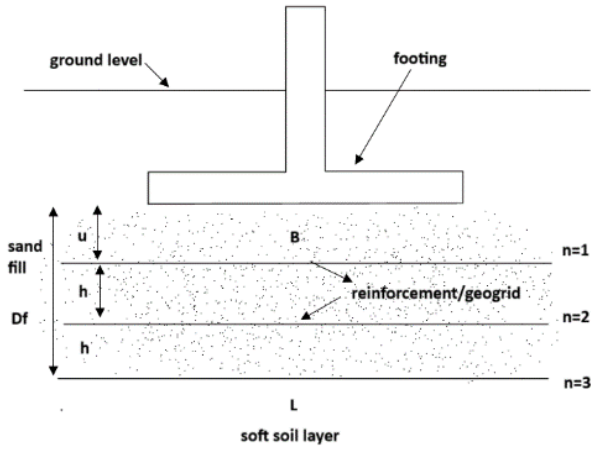

Figure 2.3 Typical diagram of geogrid reinforced foundation

The reinforced soil foundation (RSF) is a technique of placing one or more layer of geosynthetic reinforcement beneath the foundation. This concept of reinforced soil foundation emerged from late 1960_s through experimental and analytical research. This has laid foundation for evolution development of reinforced soil system. In modern context, the reinforced soil foundation (RSF) system involves replacing the weak subsoil and placing of compacted granular fill with geogrid layers at specified positions, and then construction of the footing on the improved subsoil system. Figure 2.3 shows typical arrangement of geogrid reinforced foundation with geogrid configuration.

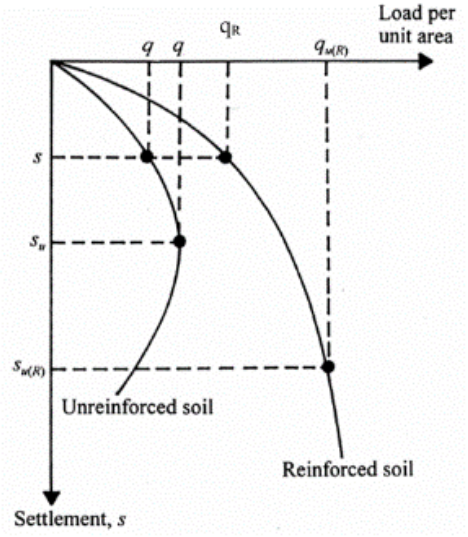

(Arab et al., 2017)

Figure 2.4 Load-settlement curve for reinforced and unreinforced foundation.

The reinforced soil foundation (RSF) is a technique of placing one or more layer of geosynthetic reinforcement beneath the foundation. This concept of reinforced soil foundation emerged from late 1960_s through experimental and analytical research. This has laid foundation for evolution development of reinforced soil system. In modern context, the reinforced soil foundation (RSF) system involves replacing the weak subsoil and placing of compacted granular fill with geogrid layers at specified positions, and then construction of the footing on the improved subsoil system. Figure 2.4 illustrates that the load carrying capacity of geogrid reinforced foundation increases and settlement reduces as compared to unreinforced foundation. The key geometric parameters influencing the performance of RSF are: the depth of placement of first geogrid layer(U), the length of the reinforcement layer (L), number of reinforcement layers (N), the vertical spacing between reinforcement layers (h) and stiffness of geogrid. These parameters are usually expressed in the dimensionless ratio normalized by width of footing (B).

2.5 Reinforcement Mechanism of Geogrid Reinforced Footing

There is various theory that explain the mechanism of geogrid reinforcement. Some of the well-established classical and modern mechanism are explained and discussed below.

2.5.1 Lateral Restrain Effect

The lateral restrain effect is one of the primary mechanisms that enhances the soil performance. It is mainly due to interlocking of soil particles within the apertures of geogrid. When the load is applied to the foundation, the soil particles tend try to move outward and deform laterally Geogrid placed below the footing acts as semi-rigid horizontal layer which restrict lateral soil movement, modifies stress distribution, changes stress path. The reinforcement also pushes the development of failure surface further deeper and also redistribute the vertical stress laterally enhancing the resistance to bearing load. In geogrid reinforced soil, grid structure plays crucial role as it effectively restrict soil displacement and further enhances confinement (Guido et al., 1986). This action consequently enhances the bearing capacity of reinforced soil system.

2.5.2 Membrane Effect

“Membrane effect” refers to the ability of a geosynthetic sheet to mobilize tension forces in reinforcement layer as it deforms with the soil under load application. When the load is applied, geogrid deforms due to which tensile stress is developed

along its length. This tensile force generates an upward reaction force that counteracts the applied load reducing the net load transmitted to underlying weak soil known as membrane effect(Chen & Abu-Farsakh, 2015). The magnitude of tensioned membrane effect is mainly governed foundation settlement, tensile stiffness of geogrid. Figure 2.5(d) illustrates this effect on geogrid reinforced foundation.

2.5.3 Stress Dispersion Effect

Footing load generates a stress bulb beneath the foundation which gradually reduces with the depth below foundation. Stress dispersion effect refers to how reinforcement layers redistribute the footing load. This effect result in formation of wider pressure bulb and lower stress concentration beneath the footing.(Guido et al., 1986) as a result vertical stress in weaker soil layer is greatly reduced, leading to lower settlement and increased bearing capacity. The stress dispersion effect can be better visualized in figure 2.5(a), as there is widening of loaded area. This widening contributes to higher bearing capacity.

2.5.4 Deep Footing Effect

The deep footing effect becomes operative when the spacing between reinforcement layer is small and the length is very short or equal to footing width, deep footing effect can be formed.(Guo et al., 2020). This effect means that the performance of reinforced soil foundation is similar to that of unreinforced foundation with an addition embedment depth equal to depth of reinforced zone(Chen & Abu-Farsakh, 2015). Figure 2.5(b) illustrates that deep footing effect.

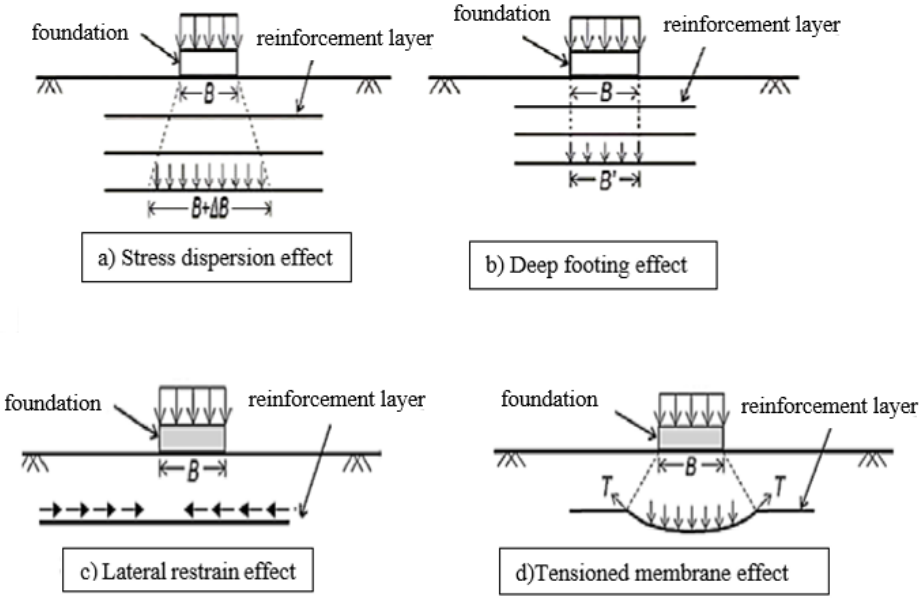

Figure 2.5 Mechanism of geogrid reinforced foundation(Arab et al., 2017)

The mechanism described above do not function in isolation in fact they operate simulate simultaneously. The interface friction is mobilized first at small deformation. As the deformation increases, passive resistance which causes lateral confining of soil mass, thus increasing the strength and stiffness of soil. If the load continues till failure, geogrid intercept shear zone and increases load carrying capacity as compared to unreinforced soil. However, the contribution of each mechanism varies with soil type, applied stress, geogrid types and configuration and magnitude of deformation.

2.6 Effect of Geogrid on Geotechnical Parameters

Geotechnical parameters govern the behavior of soil under applied load. These parameters govern the design of foundation, embankment and other civil engineering infrastructures. The effect of geogrid on geotechnical parameters are listed below:

a. Bearing capacity:

It simply refers to the maximum load per unit area resisted by soil without shear failure. Geogrid reinforcement substantially increases bearing capacity of soil through soil confinement and stress redistribution. The bearing capacity can and soil type(Albuja-Sánchez et al., 2023).

b. Settlement characteristics

Settlement is the vertical deformation of soil under load application. Geogrid reduces and limit vertical settlement by increasing the stiffness of the soil. Studies reveals that reduction can be reduced to 95% in reinforced systems(Alawaji, 2001).

c. Shear strength parameters

Cohesion and friction angle are the important shear strength parameters. These parameters represent soil resistance to failure under load. Experiment and research have shown that soil friction angle and shear strength increase due to geogrid reinforcement.

d. Stiffness

The resistance of soil to deformation is known as stiffness. The stiffness of soil increases significantly in geogrid reinforced foundation.

2.7 Experimental Investigation on Geogrid Reinforced Foundations

This section summarizes the experimental investigation carried out by several researchers with their key findings of behavior of geogrid reinforced foundation.

2.7.1 Early Investigations

(Guido et al., 1986) were among the early researcher to carry out the systematic investigation on the effect of geogrid layers on shallow foundation performance. They performed laboratory model test on geogrid reinforced square footing on sand. They proposed that the improvement in soil performance is primarily due to stress dispersion effect.

This investigation was further extended to square and strip footing by (Omar et al., 1993).They conducted parametric study and concluded that maximum bearing capacity was observed for effective reinforcement depth of 2B and 1.4B for strip and square foundation respectively and the first layer of placement of geogrid should be at depth less than B from footing base for effective reinforcement utilization. Maximum bearing capacity ratio was attained for width of reinforcement equal to 8B for strip foundation and 4.5B for square foundation, where B is the width of footing.

2.7.2 Effect of geogrid and sand fill combination

The performance of strip footings on geogrid reinforced sand over soft clay reinforced was investigated by (El Sawwaf, 2007).He found that footing performance was significantly improved with the inclusion of geogrid within the replaced sand fill compared to sand fill alone, and also found that the thickness of sand fill required to achieve allowable settlement was substantially reduced. This finding supports the use of geogrid reinforcement for ground improvement over weak soil condition.

(Latha & Somwanshi, 2009) performed both laboratory and model test and numerical analysis using finite element method on square footing placed over geosynthetic reinforced sand. They observed that reinforcement configuration and layout are crucial than tensile strength of reinforcement for bearing capacity improvement. Optimum spacing between reinforcement layer was found to be about 0.4B. Their numerical results were in good agreement with experimental results thus validating the applicability and reliability of finite element analysis.

Similarly, laboratory model tests performed to study effect of placing thin sand layer on top and placing geogrid at different depth on silty clay soil by (Kolay et

al., 2013) revealed that improvement in bearing capacity of 44.44%, 61.11%, 72.2% was obtained for two, three and four geogrid layer respectively, maintaining u/B and h/B ratio of 0.33.

Numbers of large-scale field test conducted by replacing natural clay soil with granular fill layer and placement of geogrid layer in between granular fill revealed that both granular fill and geogrid have considerable effect on bearing capacity and on subgrade modulus. They also concluded that at large strain geogrid layer are mobilized and geogrid reinforcement reduces the thickness of fill layer(Demir et al., 2013).

2.7.3 Recent Experimental and numerical studies

(Makkar et al., 2017) investigated the behavior of square footing on geogrid reinforced sand and evaluated Bearing Capacity Ratio (BCR) at a specified settlement level rather than at ultimate load which is practically more relevant performance indicator for design of foundation where settlement governs. This approach is adopted in the present study for quantifying improvement bearing capacity.

Field test was validated by numerical analysis conducted by(Demir et al., 2014) using Plaxis 3D of circular footing on geogrid-reinforced granular fill underlain by soft clay. He concluded that use of compacted granular fill layer significantly improves bearing capacity, reduces lateral and vertical displacement. For fill thickness 0.67D and N=1, (where D is diameter of footing and N is number of reinforcement layer) optimum reinforcement location was observed between 0.1D-0.5D below footing yields 90% increase in bearing capacity and settlement reduction of 53%. They also stated that adding a second layer of geogrid between 0.15D-0.3D below first layer improved bearing capacity by 230% and reduced settlement by 60%.

Similarly, a series of model test was conducted by (El-Attar & El-Latief, 2024) to study performance of square footing on geogrid reinforced soft clay. They compared the result obtained from experimental model with result obtained from finite element program ABAQUS which were in good agreement. They found that placement of first geogrid layer u=0.7 was appropriate to improve soft clay property. They stated that minimum geogrid length should be 3B where B is width of footing to reduce consolidation settlement and geogrid were found ineffective in reducing creep settlement.

Small-scale laboratory test of strip foundation on reinforced geogrid-reinforced sand revealed that bearing capacity ratio at ultimate load was greater than ultimate load (Shin et al., 2002).

2.8 Numerical modeling by PLAXIS 3D

The physical condition of engineering problems often described by numerical models. It has become most efficient tools for analysis of soil-reinforcement interaction that are usually not fully captured by using analytical and experimental studies. PLAXIS 3D is a powerful and user-friendly finite element-based software which can be used to solve many geotechnical problems. It can be used for deep excavations problems, foundations, tunnels, and retaining structures for both analysis and design purpose. It solves complex differential equations to obtain solution for complicated engineering problems. Plaxis3D has inbuilt features that allows to create geogrid element. There are various constitutive models available in Plaxis like Mohr-coulomb, Hardening soil models that enables accurate modelling and capturing of geogrid-soil interaction,

Finite Element Method have been used by (Abdolhosseinzadeh et al., 2022) for numerical analysis of bearing capacity of circular foundation reinforced with geogrid. Similarly(Abu El-Soud & Belal, 2019) have modelled strip foundations overlaying geosynthetic-reinforced loose fine sand deposit and was validated with experimental results.

The FEM has many advantages of its own. Some of them are given below:

1. FEM is versatile and complex geometries can be easily modelled.
2. This method enables distinct characterization of materials.
3. It can be adopted to meet specific requirement.
4. The method is suitable to handle irregular boundary condition and also ensure realistic simulation
5. The effect of material anisotropy and inhomogeneity can be easily accommodated.

3 METHODOLOGY

This section presents a summary of overall methodology applied for the complete analysis and presentation of the result. The entire process is clearly explained with the help of a flow chart as shown below in Figure 3.1.

a. Literature review and data acquisition: The primary objective is to review existing literatures and to identify research gap on the research topic. Another motive is to obtain the input data required for FE software. Most of the parameters are obtained through secondary source along with literature review to find correlation for processing of acquired data to obtained ready to use input data.

b. Processing of data for input: Data acquired from step a, is processed with consideration of the empirical relation as well as mathematical relation from different books and literatures to obtain modelling input data ready.

c. Numerical Modelling: Acquired data is processed using several empirical correlations and mathematical relation to obtain modelling input data ready

d. Model calibration and validation: The result obtained from FE model is compared with existing field result and calibration is done to assure the accuracy of model.

e. Parametric study: A number of parametric study is conducted by further extending the valid model to investigate the influence of several geogrid parameters on the performance of geogrid reinforced shallow foundation.

f. Result and Discussion: The output obtained from numerical analysis is expressed in terms of load settlement curves, BCR and SRF.

g. Conclusion and Recommendation.: Finally, the conclusion of the research is presented and recommendation for future work is presented.

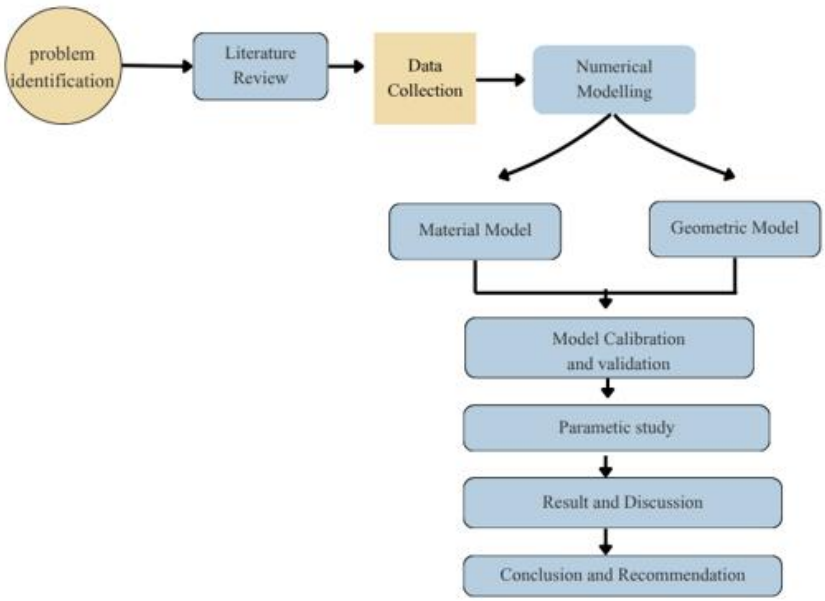

Figure 3.1 Methodology

3.1 Material Model

3.1.1 Soil Constitutive Model

Soil constitutive model in geotechnical engineering is a mathematical framework that describe mechanical response of soil under loading and deformation condition. Soil is complex material that shows non-linearity, anisotropy, time dependent effect and also irreversible behavior under stress. Constitutive model is designed such a way so as to capture this behavior by formulating equation or algorithms that establish relationship between stress and strain under various loading conditions. There are many types of constitutive soil models and every model differs in their functionality. Some of common soil constitutive models are:

a) Elastic Model: This model assumes that soil behavior is linearly elastic which means that there is linear stress and strain relationship. Pure elastic models are useful only for small deformation since soil usually shows non-linear behavior at higher strain. Linear elastic and nonlinear elastic are the examples of linear elastic model.

b) Plastic Model: These model focuses on plastic deformation and usually incorporate yield surface. It specifies upper threshold limit above which the plastic deformation starts to develop. Examples are Cam-Clay model .
c) Elastoplastic Model: This model is the combination of both elastic and plastic model. It accounts for plasticity for higher strain and elasticity for lower strain. A well-known example of elastoplastic model is Mohr-coulomb model.
d) Critical State Model: This model is based on the concept of critical state, which refers to the condition at which soil reaches its maximum density and shear strength. These models are mostly used for sand and gravel as they describe behavior of soil at critical state.
e) Hyperplastic Models: Mostly used for soft soil that undergo large deformation. Behavior of organic material and peat soil are often represented by this model.

3.1.2Mohr-Coulomb model

Mohr-Coulomb model is simple, linearly elastic perfectly plastic model, which are generally used for first approximation of soil behavior. It is a constitutive model which describes shear strength and failure behavior of coarse and fine-grained soil. It. involves five input parameters, E and ν for soil elasticity, ϕ and c for soil plasticity and ψ as an angle of dilatancy. The Mohr-Coulomb model relates shear stress(τ) and normal stress (σ_n) on failure plane using following equation:

$$\tau=c+\sigma_n*\tan(\varphi)$$

Where: τ is the failure plane's shear stress. φ is the angle of internal friction.

c is the cohesion of the soil.

σ_n represents the normal stress applied to the failure plane.

As per Mohr-coulomb theory, the soil failure occurs when the shear stress acting on a plane exceeds its shear strength. The shear strength of the soil is governed by cohesion and the angle of internal friction. The Mohr Coulomb model is an easy to use yet effective way to analyze, bearing capacity of foundations, soil stability, and other geotechnical engineering problems. However, for the model to perform accurately it is very essential to obtain accurate Mohr-Coulomb parameters. Apart from these parameters, the initial condition of the soil also has a significant influence on soil deformation behavior and related geotechnical problems.

Table 3.1 parameters for Mohr-Coulomb model

Symbol	Description	Unit
E	Young's Modulus	kN/m^2
ν	Poisson's Ratio	-
φ	Friction Angle	°
c	Cohesion	kN/m^2
ψ	Dilatancy Angle	°

3.2 Acquisition of Soil Parameters

The SPT test conducted for 132/11 kV Teku substation construction site at Teku, Kathmandu, Nepal. SPT test was conducted as per IS 2131-1981.SPT N value of soil was recorded at every **1.5m interval**. The test was conducted **up to** the depth of 30m.The soil profile was predominantly found to be low plastic silty soil. SPT N value of soil profile ranges from 2 to 5 and. Based on N value the consistency of soil has been identified in this study. Table 3.2 illustrates that soil is very soft too soft in nature which indicates that it may possess low shear strength and highly compressibility

Table 3.2: Variation of Consistency with N value

(Geotechnical Design Manual, 2010)

SPT N value	Consistency
0 -2	Very soft
2-4	soft
4-8	Medium
8-15	stiff
15-30	Very stiff
>30	Hard

The parameters required for numerical modelling were acquired through soil investigation report and some parameters were determined and obtained using mathematical relationships developed and suggested by various researchers.

Table 3.3:Typical value of Young's Modulus (Mpa) (Obrzud & Truty, 2018)

USCS	Very soft to soft	Medium	Stiff to very stiff	Hard
ML, CL	1.5-6	6-10	10-30	30-60

Above table 3.3 illustrate the typical range of soil young's modulus based on soil classification and its consistency. Since the soil considered in this study is low plastic silt so the young's modulus of elasticity is adopted in range between (1.5-6) Mpa. For numerical analysis 2.2 Mpa was adopted.

Table 3.4: Value range for Poisson's ratio, ν (Bowles, 1996)

Type of soil	ν
Saturated clay	0.4 – 0.5
Clay, unsaturated	0.1 – 0.3
Sandy clay	0.2 – 0.3
Silt	0.3 – 0.35
Sand, gravelly sand	0.3 – 0.4

The value of poison's ratio is adopted as 0.3 for silty soil. The dilatancy angle ψ, is specified in degrees and represent volumetric expansion of soil during shear deformation. Usually, fine grained soil exhibits limited dilation during shearing. Except for highly over-consolidated clay layers, clay soil normally shows negligible dilatancy. In sandy soils, the dilatancy behavior is mainly governed by friction angle and relative density of sand. When friction angle of soil exceeds 30°, dilatancy angle can be computed by using $\Psi = \varphi - 30°$,

However, for sands with φ less than 30°, the dilatancy angle is generally taken as zero. Since the low plasticity silty soil exhibits negligible dilation characteristics, dilatancy angle was taken as 0^0. The summary of soil parameters considered for the study are tabulated below:

Table 3.5: Parameters considered in soil model

Depth	Thickness	Y_{dry} (kN/m^3)	Y_{sat} (kN/m^3)	C (kN/m^2)	φ	ν	E (kN/m^2)	ψ
0-1.5	1.5	13.24	17.55	5	23	0.3	2200	0
1.5-9	7.5	13.53	16.48	4	21	0.3	2200	0

3.3 Acquisition of Foundation Parameters

The foundation was modeled as plate element available in Plaxis 3D.Foundation plate element unit weight, young's modulus of elasticity and poisons ratio were derived from (Makkar, 2022).

Table 3.6: Foundation Material Properties

Parameter	Values
Size of plate/ footing (m)	0.45*0.45
Unit weight of plate (KN/m^3)	78.5
Youngs modulus of Elasticity(E)	200*10^6
Equivalent Thickness of plate, m	0.025
Poisson's Ratio	0.3

3.4 Acquisition of sand fill parameters.

The empirical formula developed by(Benz & Nordal, 2010) for sand has been used to determine property of sand used in this study.(Emirler et al., 2019) also used same empirical formula to derive sand property to conduct 3D Numerical Response of Single Pile under Uplift Loading Embedded in sand. The relative density (RD)of sand has been used to determine various sand property as illustrated below.

$\gamma_{unsat} = 15 + 4.0\,RD/100\ \ (kN/m^3)$ Equation 3-1

$\gamma_{sat} = 19 + 1.6\ RD/100$ Equation 3-2

From Eq (3-1) & (3-2) the unsaturated and saturated unit weight can be calculated by assuming relative density of sand.

$E^{ref}_{oed} = 60000\,RD/100\ \ (kN/m^2)$ Equation 3-3

$E = ((1+\nu)*(1-2\nu)/(1-2\nu))*E^{ref}_{oed}\ (kN/m^2)$ Equation 3-4

$\varphi = 28 + 12.5\,RD/100$ Equation 3-5

$\psi = -2 + 12.5\,RD/100$ Equation 3-6

For this study RD of 30% for loose and 50% for medium dense sand is assumed. Modulus of elasticity of sand can be obtained from Equation 3-3 & 3-4 and sand friction angle and dilatancy can be obtained from Equation 3-5 and 3-6 by simply entering the relative density of sand.

Table 3.7:Property of sand used in this study

Relative density (R.D)	Loose Sand (RD=30%)	Medium sand (RD=50%)
Material model	Mohr-coulomb	Mohr-coulomb
Drainage type	Drained	Drained
γ_{unsat} (kN/m^3)	16.2	17
γ_{sat} (kN/m^3)	19.5	19.8
E(kN/m^2)	15000	25000
φ	32	35
ν	0.25	0.25
ψ	2	5
C (kN/m$^{2)}$	0	0

3.5 Geogrid parameters

The geogrid is modeled as linear elastic element using geogrid inbuilt feature available in Plaxis 3D. The parameters of the numerical model are expressed in table 3.9.

Table 3.8: Geogrid used in this study

Geometrical Parameters	Values
Axial Stiffness (EA)	500kn/m in both direction (tensar)

3.6 Geometric Model

To develop Finite element model, it is essential to accurately define the overall model geometry apart from defining material parameters. This section explains about model geometry adopted, boundary condition of prepared model, meshing and calculation process.

3.6.1 Model Geometry

The geometry of model plays important role in numerical simulation. In numerical analysis of geogrid reinforced foundation appropriate selection of model boundary is crucial to ensure that computed results are free from boundary

induced distortions. The model dimension was selected in such a way that there will be very less strain near the boundary. The length, width and height of model was considered as 20 B (twenty times the size of footing) in this study as shown in figure 3.2.

The main purpose behind adopting such a large model domain is to minimize the influence of artificial boundaries on stress distribution and deformation behavior below the footing. If the boundaries are located too close to the loaded region, they tend to restrain lateral displacement and modify stress paths, which may lead to unrealistic predictions of bearing capacity and settlement. By extending the model boundaries sufficiently far from the footing, these undesired effects can be effectively avoided (Potts & Zdravko Vic, 2001).It has been reported in the literature that the significant stress influence zone beneath shallow foundations generally extends to a distance of about 4B–5B laterally and 2B–3B in depth, depending on soil properties and loading conditions(Das, 2011). Therefore, selecting a model width of 20B ensures that the boundaries are well beyond the zone of influence, allowing for a more realistic representation of soil behavior. Furthermore, in the case of geogrid-reinforced foundations, the load transfer mechanism involves additional factors such as tensile membrane action and soil–reinforcement interaction, which may extend the zone of influence beyond that of unreinforced soil. This necessitates the use of relatively larger model dimensions to capture the true behavior of the reinforced system.

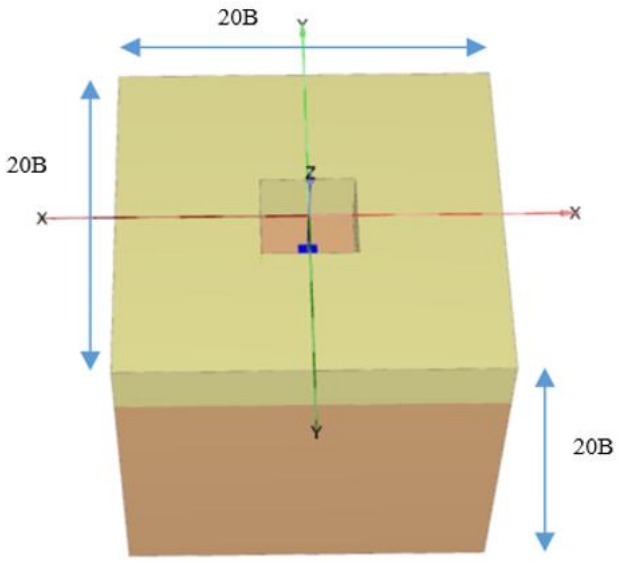

Figure 3.2: Geometry of soil model

Based on these considerations, the selected model geometry of 20B is deemed appropriate for the present analysis, as it ensures minimal boundary interference

while accurately capturing the stress distribution, settlement characteristics, and reinforcement behavior.

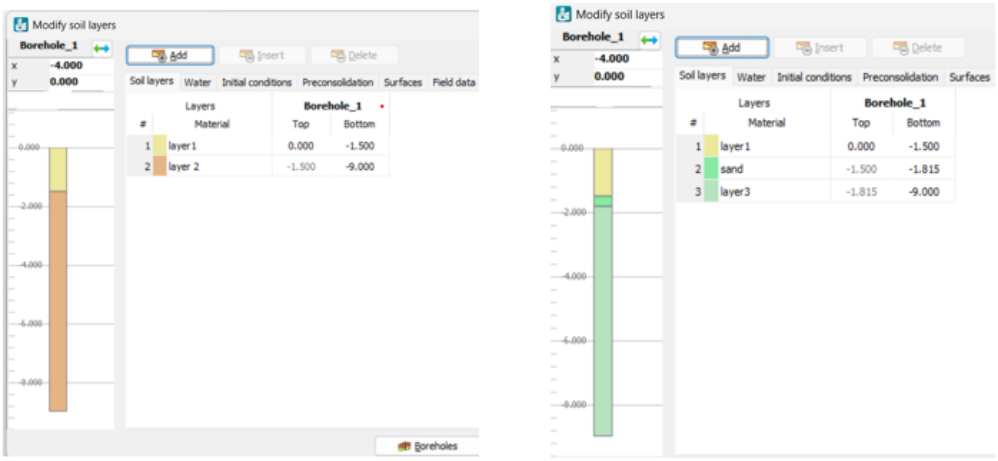

(a) (b)

Figure 3.3: Unreinforced (a) and Reinforced (b) borehole logs

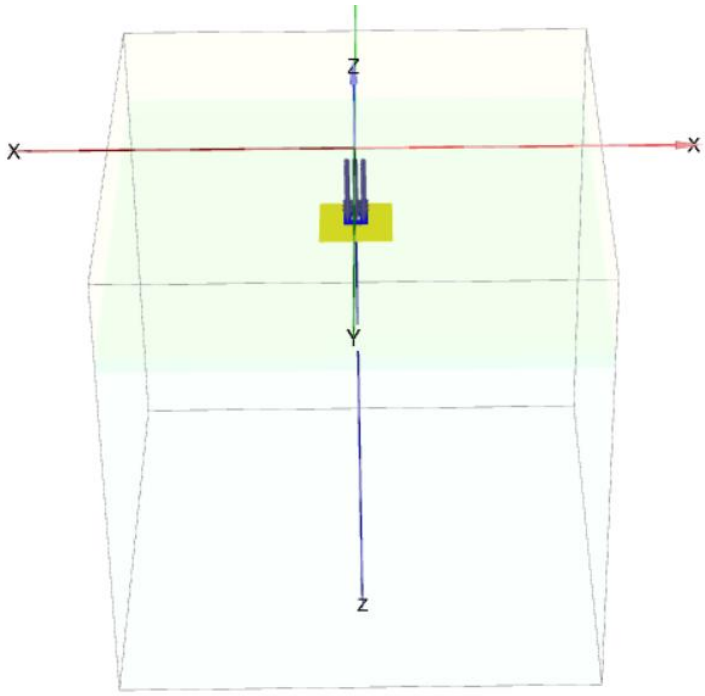

Figure 3.4: Figure showing arrangement of load and geogrid

Table 3.9: Geometric parameters of model

Geometrical Parameters	Values
Footing width (B)	0.45m (B)
Width of a soil	20B (9m)
Depth of analysis soil	20B (9m)
Embedment depth of footing	1.5m

3.6.2Boundary condition

FEM based program relies on iterative procedure to analyze stress and strain induced in the model, gradually approaching to a solution that satisfies model boundary condition. It defines how model will respond during the loading. Therefore, it is very important to define model boundary in order to reflect actual site condition. In present analysis horizontal and vertical movements were restrained at the bottom boundary, while the vertical boundary were normally restrained. The top surface of soil was kept free so that the ground response due to applied load can be properly evaluated

3.6.3Meshing

Generation of finite element mesh is an important step for smooth and accurate calculation. The mesh should have good quality which means the element should be of proper shape and should not be excessively elongated or distorted. Smaller elements are generally required in regions where large variations in stress and strain are expected during the analysis. However, it is not necessary to use very small elements throughout the entire model, as an excessively fine mesh increases computational effort and analysis time. Proper meshing also helps in improving the convergence behavior of the numerical model and reduces the possibility of numerical instability during computation. Therefore, an optimum balance between mesh refinement and computational efficiency should be maintained to achieve accurate results within reasonable analysis time. Ten-nodded tetrahedral elements were generated for soil materials and six-nodded element for plate and geogrid. Medium mesh with enhanced mesh refinement was done at footing area.

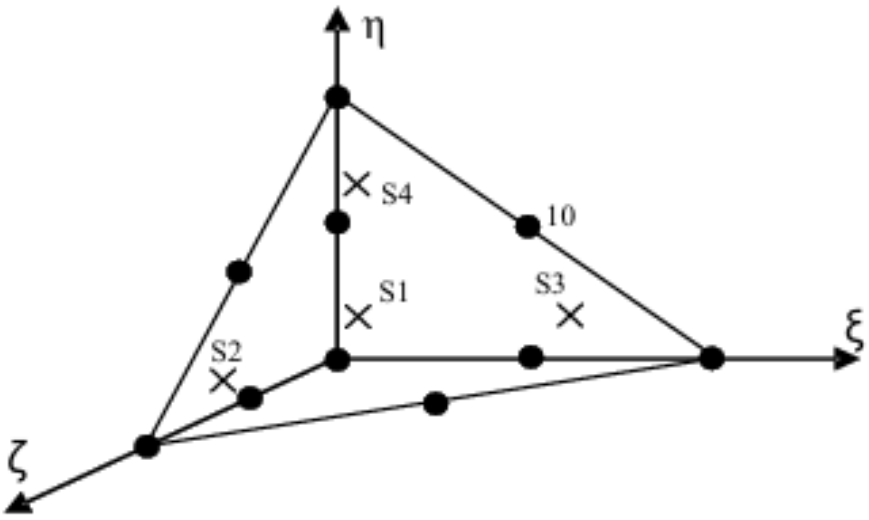

(-PLAXIS-3D-2024-1-3D-2-Reference-Manual, n.d.)

Figure 3.5: 10-node tetrahedron soil element

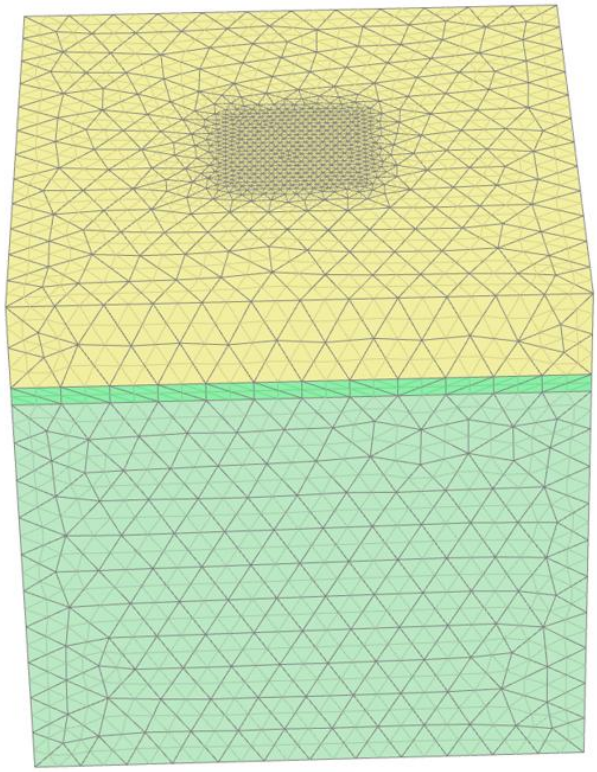

Figure 3.6 Generated mesh of soil mode

3.7 Numerical calculation

Calculation process in PLAXIS 3D is divided into several calculation phases. Initially model geometry, soil and material parameters are assigned and meshing is done calculation phase is started. In calculation or staged construction phase various parameters are activated or deactivated in accordance with the purpose of study. Once the complete model geometry and meshing is completed. The first phase also known as initial phase which calculates the initial stress was generated by using K_0 procedure. After this phase excavation phase, is activated which excavates the soil volume for foundation. Then the plate installation phase is activated which places the plates at respective position as defined in the model. Finally, loading phase or prescribed surface settlement phases were simulated. The calculation type was selected as plastic. An equal amount of load as that of the field plate load test was applied to measure the settlement at the corresponding load to study the reduction in settlement. Prescribed surface displacement of 25 mm was simulated, and the pressure corresponding to different settlement levels was recorded to measure improvement in bearing capacity.

Once the model was completed, output was generated and pressure versus settlement was recorded. The improvement in settlement was analyzed based on the settlement observed at the load level corresponding to the field plate load test in terms of the settlement reduction factor (SRF). The improvement in bearing capacity were expressed in bearing capacity ratio (BCR) at different settlement levels.

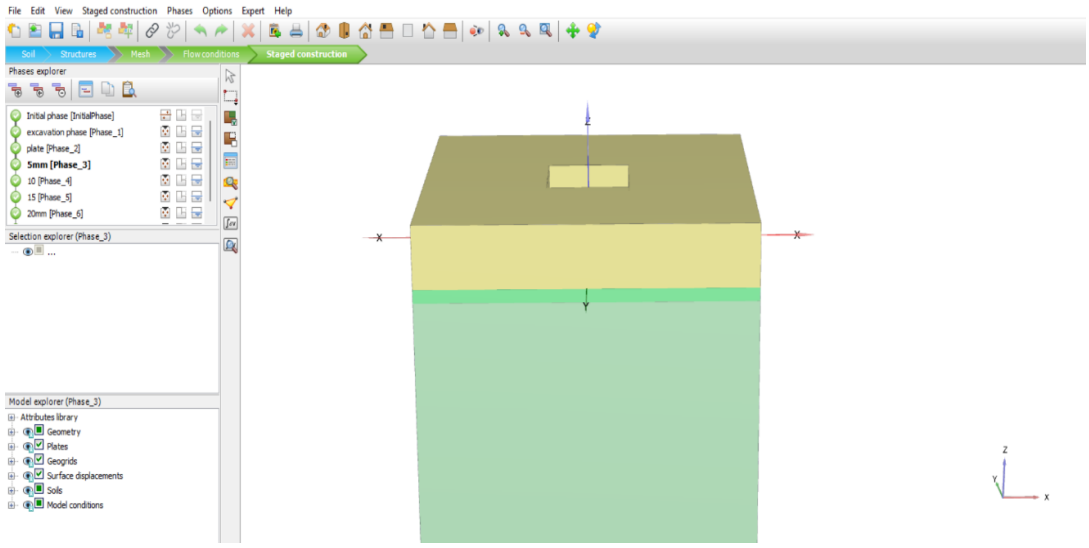

Figure 3.7 Phases of simulation

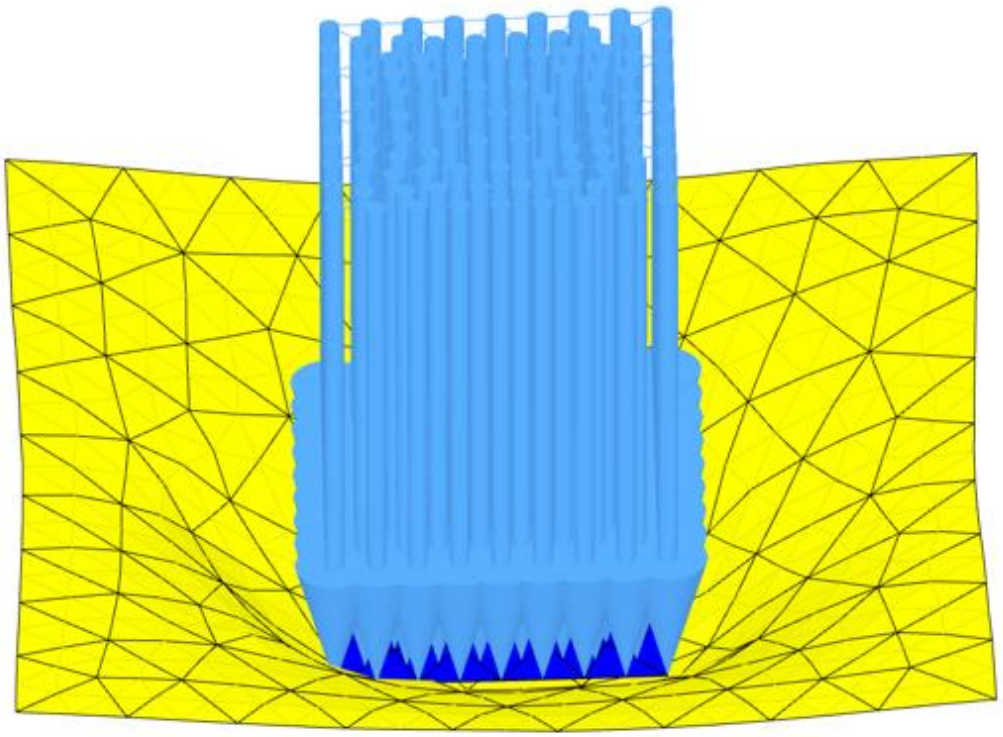

Figure 3.8: Deformed shape of geogrid under load application

3.8 Output

Output results from parametric study are analyzed and load settlement curves were plotted. From the load-settlement curves, the bearing capacity is obtained. The improvement in bearing capacity have been quantified by using non-dimensional parameter as used by (Makkar et al., 2017) Bearing capacity Ratio (BCR),which can be expressed as the ratio of bearing pressure of unreinforced soil to that of reinforced soil

$BCR=q_R/q_o$

Where, q_R is the bearing pressure of reinforced soil at a given settlement level

q_o is the bearing pressure of unreinforced soil at same settlement level.

In this study BCR ratio is calculated at different settlement level. The improvement in footing settlement was quantified through settlement reduction factor (SRF) which is the ratio of difference in settlement of unreinforced and reinforced footing to settlement at reinforced footing at same settlement level. It can be expressed as

$SRF=(S_0-S_r)/S_0$ Where, S_0 is the settlement of unreinforced footing and S_r is the settlement corresponding to reinforced footing at same pressure.

3.9 Model Validation

Model validation is the process of determining how accurately the model performs in reality. In this study Pressure Vs displacement response from FEM and Field plate load tests of unreinforced soil are compared in figure 3.9. It was observed pressure Vs settlement curve of FEM simulated plate load test closely matches to field plate load test result with an error of 4.96% in settlement at load of 19.62 KN (96.89 KN/m^2) as shown in Table 3.10 which implies the model has performed satisfactorily and thus the model is validated.

Table 3.10: Fem & Field Load Vs settlement data

Description	Load (kN)	Pressure (kN/m^2)	Settlement (mm)	Error (%)
Field plate load test	9.81 19.62	48.44 96.88	-6.5 -25	
Fem simulated plate load test	9.81 19.62	48.44 96.88	-8.24 -23.83	4.68%

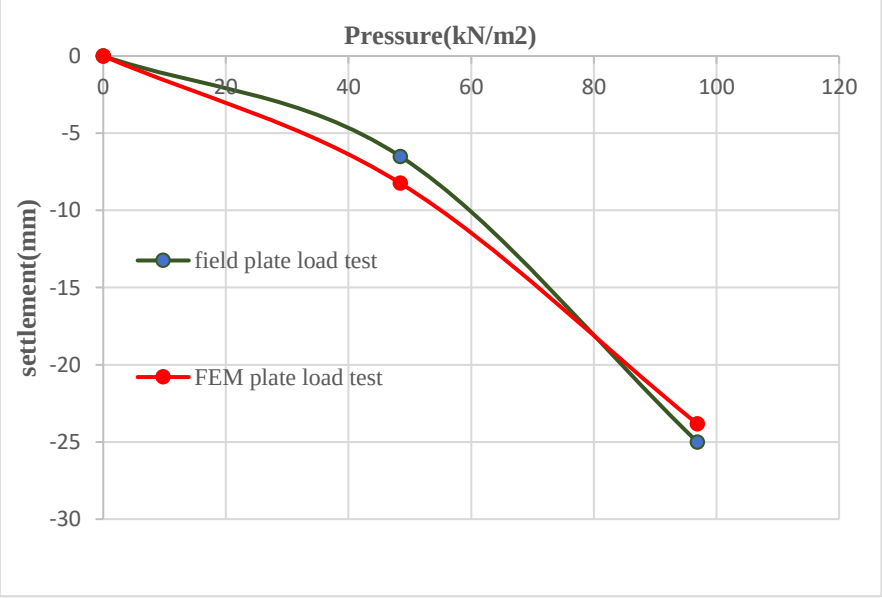

Figure 3.9 FEM Vs Field plate load test curve.

3.10 Parametric study

The validated model was further extended, and a parametric study was conducted by varying geogrid configuration, thickness, and sand fill property to analyze the behavior of geogrid-reinforced footing.

Table 3.11 Parameters considered for parametric study.

Series Name	Constant parameters	Variable parameters
a) To find optimum placement of first geogrid layer(u)	d/B=0.7, N=1, L/B=3, RD=50% EA=500	u/B=0.1,0.2,0.3,0.4
b) To find spacing between geogrid layer (h)	d/B=0.7, N=2, L/B=3, u/B=0.2, RD=50%, EA=500	h/B=0.1,0.2,0.3,0.4
c) To find optimum number of geogrid layer	d/B=0.7, L/B=3, u/B= h/B=0.2, RD=50%, EA=500	N=1,2,3
d) To determine optimum size of geogrid	d/B=0.7, u/B= h/B=0.2, N=2, RD=50%, EA=500	L/B=2,3,4
e) To investigate effect of depth of sand fill	u/B=h/B=0.2, N=2, L/B=3, RD=50%, EA=500	d/B=0.7, 1, 1.25, 1.5
f) To investigate effect of relative density of sand fill	d/B=0.7, u/B=h/B=0.2, N=2, L/B=3, EA=500	RD=30%, 50%
g) Effect of stiffness of geogrid (kN/m)	d/B=0.7, u/B=h/B=0.2, N=1, L/B=3,	EA=250,500,750 1000,1250
h) Size of Footing	d/B=0.7, u/B=h/B=0.2, N=1, L/B=3	(0.45*0.45) m (0.75*0.75) m (0.9*0.9) m (1.05*1.05) m (1.2*1.2) m

4 RESULT AND DISCUSSION

The result from parametric study is summarized and presented below;

4.1 Optimum embedment depth of first geogrid layer

The behavior of RSF primarily depends in the location of placement of first geogrid layer. To determine the optimum depth of placement of first geogrid layer it was examined at five depth ratios (u/B=0.1,0.2,0.3,0.4 and 0.5) where (u) represent the depth of first reinforcement layer below footing and(B)represent width of footing. The load settlement response shown in figure 4.1 shows that as the depth of placement of first geogrid layer increases bearing capacity increases up to u/B ratio of 0.2 and then decreases for further increase in depth of placement of first geogrid.

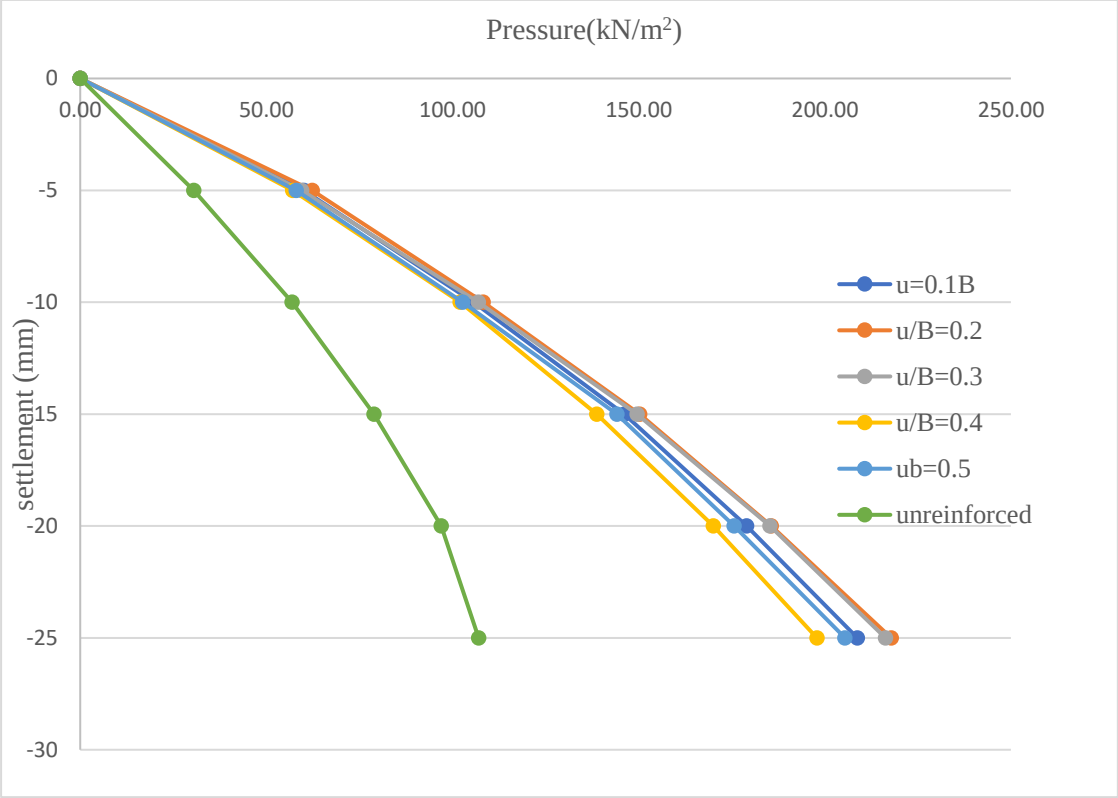

Figure 4.1:Load settlement curve for different u/B ratio

Figure 4.2 shows variation of BCR at different settlement level. It was observed that BCR increases from and attain maximum improvement at u/B 0.2-0.3 and decreases beyond u/B=0.3. However overall trend of BCR improvement remains similar. The improvement in BCR was more than twice the unreinforced foundation when first geogrid layer was placed at depth of u= (0.2 -0.3) B.

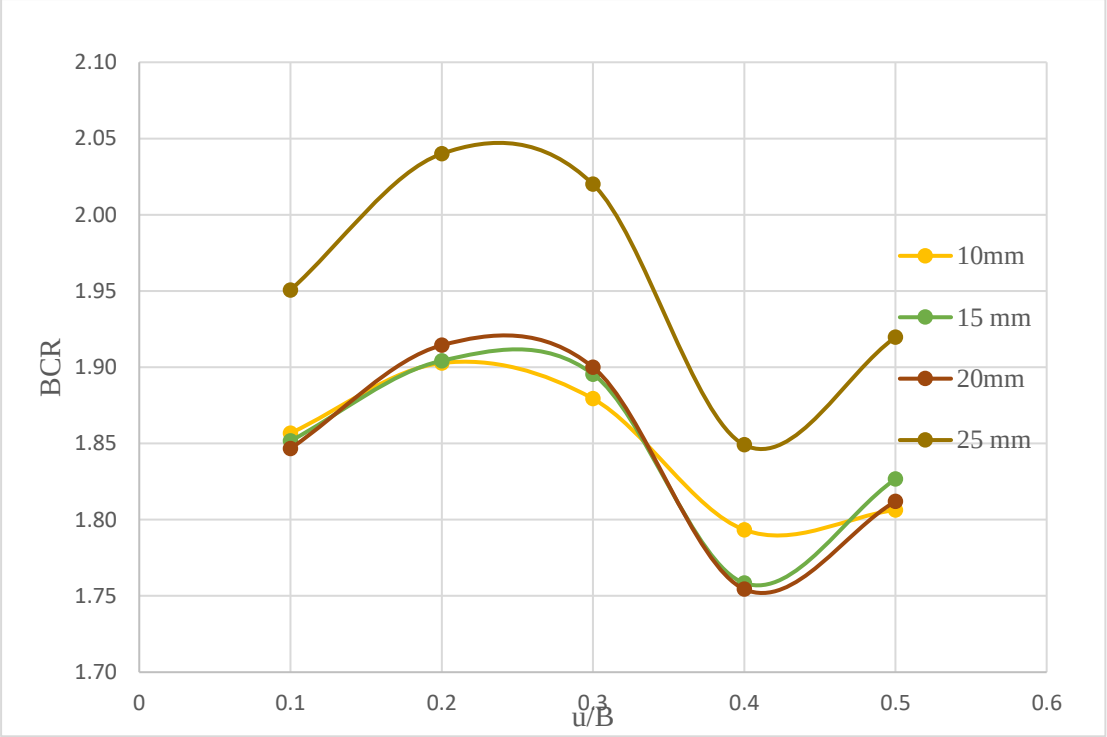

Figure 4.2 Variation of BCR with depth of placement of first geogrid layer

At this depth geogrid lies within the active failure zone, where geogrid mobilizes maximum tensile forces and increases soil confinement. This result indicates that maximum improvement in bearing capacity is attained when first geogrid layer is placed close to footing indicating effective mobilization of tension membrane effect and confinement effect.

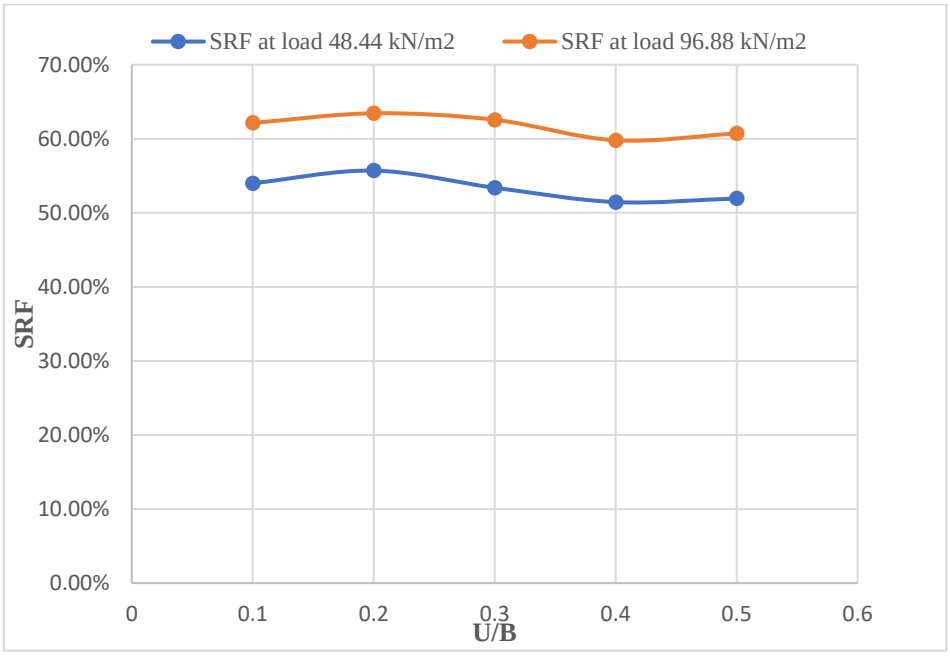

Figure 4.3:SRF at various u/B ratio

Similarly, improvement in settlement due to addition of geogrid layers were assessed by obtaining settlement corresponding to pressure of 48.44 kN/m2 and 96.88 kN/m2. It was observed that similar trend like bearing capacity was observed with improvement of 60-62 % corresponding to load value of 96.88 kN/m2 as shown in figure 4.3. On the other hand, maximum reduction in settlement is obtained when u/B ratio between 0.1-0.3 with maximum improvement at u/B ratio of 0.2. Increment of depth beyond u/B ratio of 0.3, SRF decreases slightly. This is due to the fact that effectiveness of geogrid to reduce settlement reduces at deeper reinforcement depth. Thus, from the graph it is observed that for both bearing capacity and settlement criteria optimum depth of placement of first geogrid layer was attained at u/B ratio of 0.2 to 0.3. In this study optimum placement of first layer of geogrid is considered as 0.2B.

4.2 Effect of Vertical spacing of Geogrid(h)

To investigate the effect of vertical spacing between geogrid layer the optimum depth of first geogrid layer is taken as u/B=0.2 below the footing. The spacing between geogrid layer was varied for different h/B ratio. Bearing capacity at various settlement levels are compared with unreinforced case and the result are expressed in terms of BCR. Figure 4.4 and 4.5 shows that BCR ratio increase significantly up to h/B ratio of 0.1-0.2, while moderate improvement at h/B ratio of 0.3-0.4 and decrease beyond h/B ratio of 0.4. Maximum BCR improvement of 2-2.08 was observed at (h/B =0.1 to 0.2) and BCR drops to 1.78 times the unreinforced case at spacing of 0.5.

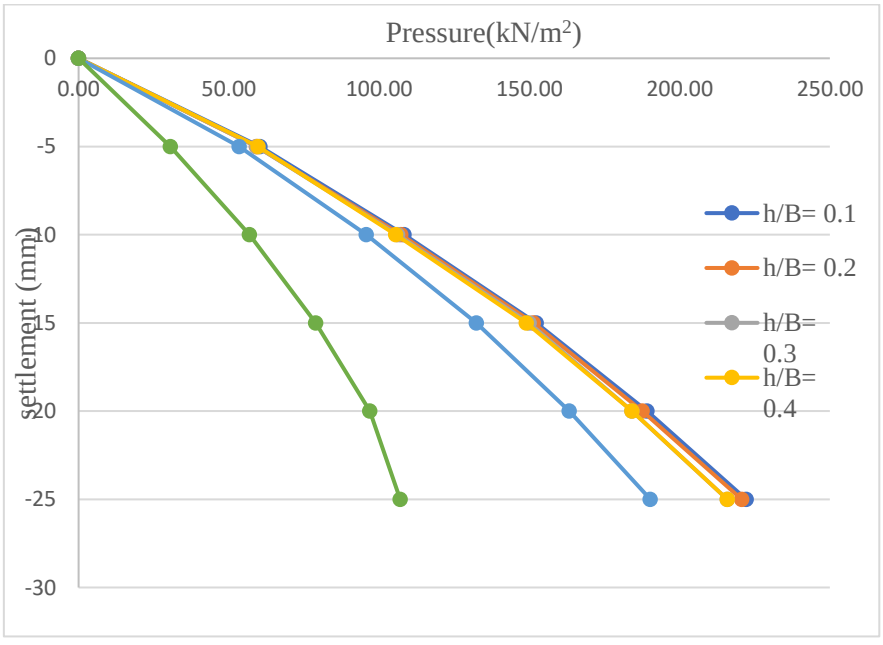

Figure 4.4:Pressure vs settlement curve for h/B ratio.

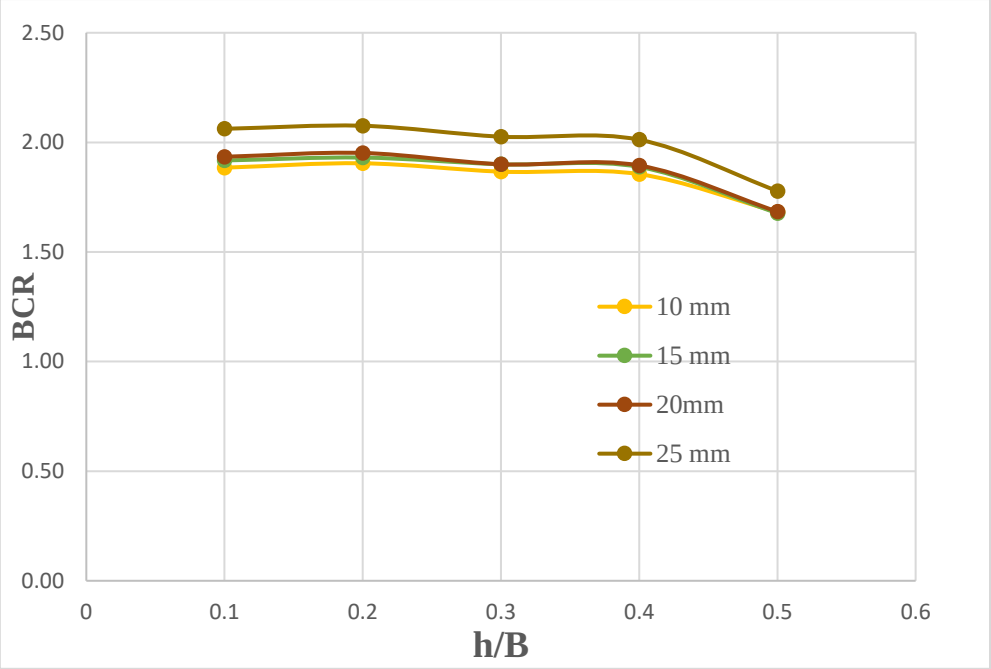

Figure 4.5: BCR at different h/B ratio

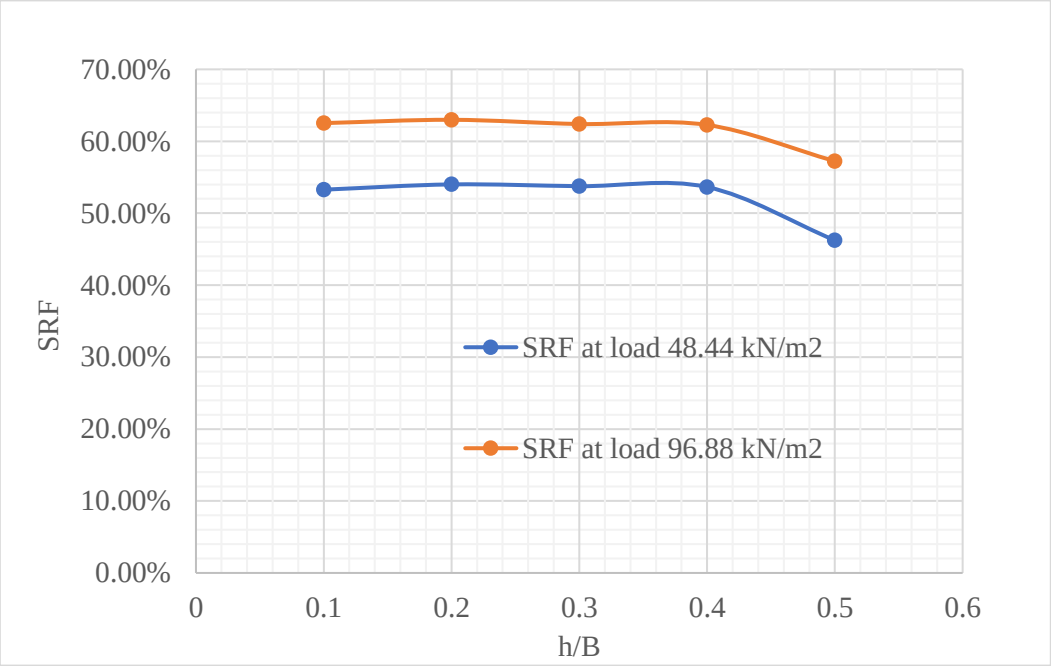

Figure 4.6: SRF at different h/B ratio

Similar trend was observed and settlement improvement of about 62% was observed at h/B ratio of 0.2. while minimum improvement of 57% was observed at h/B ratio of 0.5 at same stress of 96.88kN/m2 as observed in figure 4.6. Beyond h/B value of 0.4 both bearing capacity and improvement in settlement declines. For both BCR and SRF the optimum depth of geogrid reinforcement lies within the depth of 0.1 to 0.2. This indicates that reinforcement layer significantly contributes to load carrying capacity and reduces settlement when it is placed

within high-strain zone below footing due to the fact that reinforcement mobilizes the frictional resistance and increase load carrying capacity and minimizes settlement. Thus, with placement of first geogrid layer at optimum depth significant improvement in bearing capacity can be attained at vertical spacing of h/B ratio of 0.1 to 0.2. In this study optimum spacing between geogrid is considered as 0.2.

4.3 Effect of Number of Geogrid layer

The effect of number of geogrid layer was investigated by placing first geogrid and spacing between them at optimum depth of u/B=h/B=0.2. The inclusion of first geogrid layer significantly increases load bearing capacity, whereas with further inclusion of second and third geogrid layer minimal improvement in load capacity was observed as shown in figure 4.7.

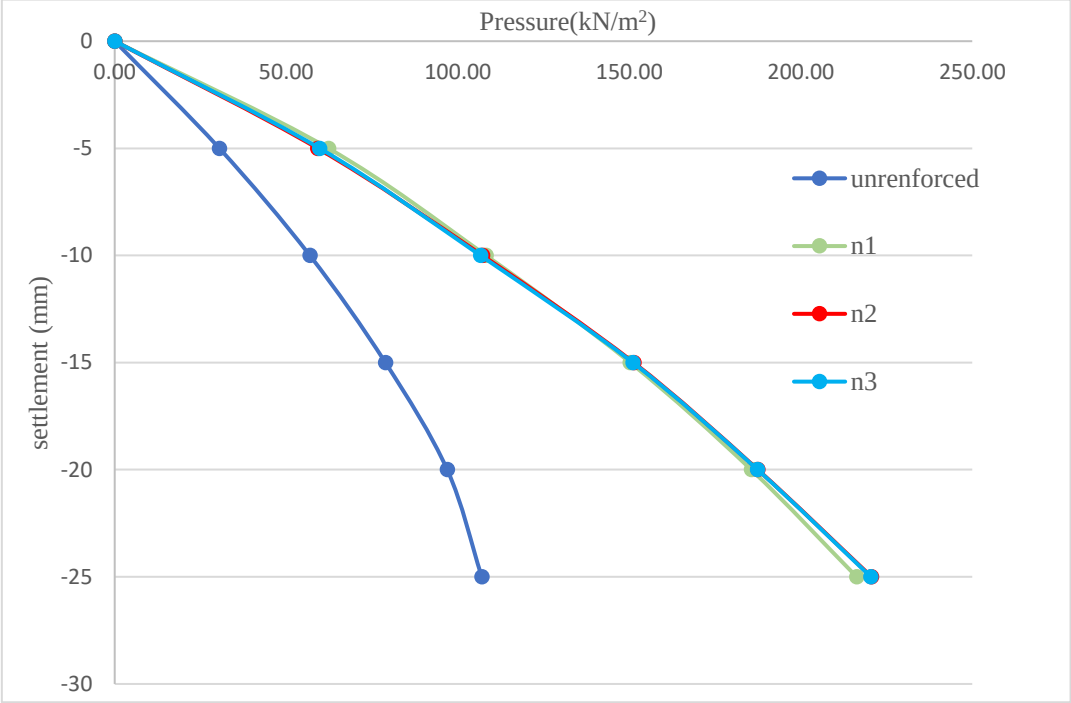

Figure 4.7: Load vs settlement curve for numbers of geogrid layer

Similarly, improvement in settlement due to addition of geogrid layers were assessed by obtaining settlement corresponding to pressure of 48.44 kN/m2 and 96.88 kN/m2. It was observed that similar trend like bearing capacity was observed with improvement of 60-62 % corresponding to load value of 96.88 KN/m2 as shown in figure 4.8.

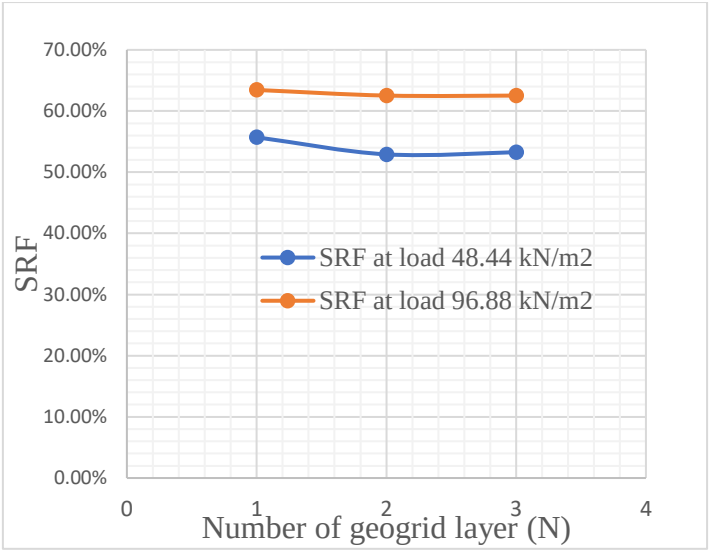

Figure 4.8:SRF for number of geogrid layer

Furthermore, the displacement contours (figure 4.9 and 4.10) for single and three-layer geogrid reinforcement shows that stress influence zone is relatively shallow and narrow for multiple geogrid reinforced foundation which has restricted soil movement to smaller zone. It was observed that first geogrid layer is effectively mobilized since it is located within maximum deformation zone while second and third layer lies near the boundary and outside the significant deformation region due to which additional layer do not experience sufficient strain to mobilize their tensile capacity effectively.

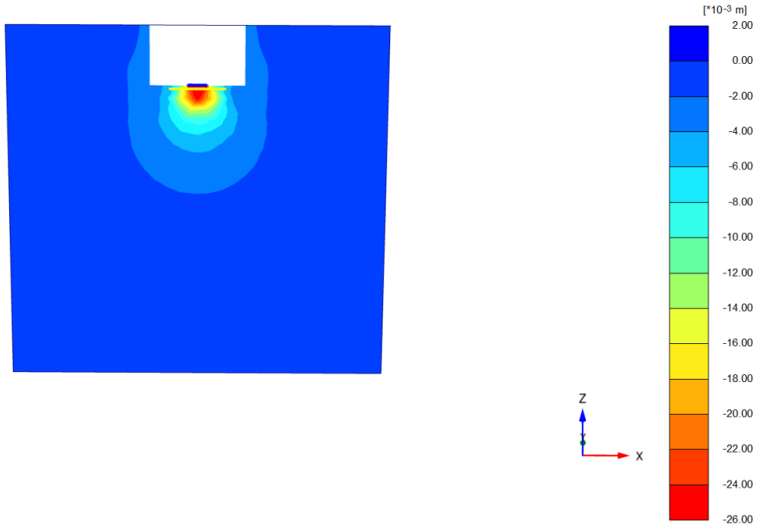

Figure 4.9 Displacement contour for single layer of geogrid reinforcement

Figure 4.10 Displacement contour for three layer of geogrid reinforcement

Figure 4.11, 4.12 & 4.13 which shows that axial force in first geogrid layer is maximum and minimum in third layer indicating first geogrid layer intercepts the peak stress and additional layer receives less stress and contribute marginally. This is also due to the fact that deeper geogrid layer experiences minimal strain at this settlement level. Furthermore improvement in bearing capacity of geogrid reinforced foundation depends upon the magnitude of settlement, with relatively smaller enhancement at lower settlement levels (Shin et al., 2002). This implies that under settlement level of 25mm there have been limited strain mobilization within lower geogrid layer, leading to reduced load bearing capacity.

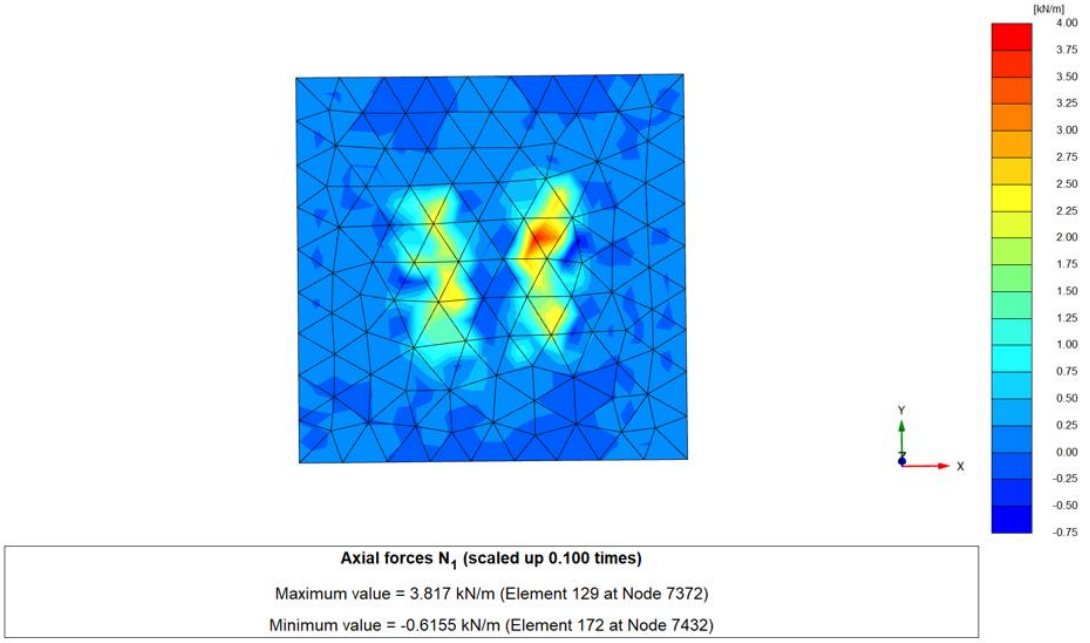

Figure 4.11 Axial force in first geogrid layer

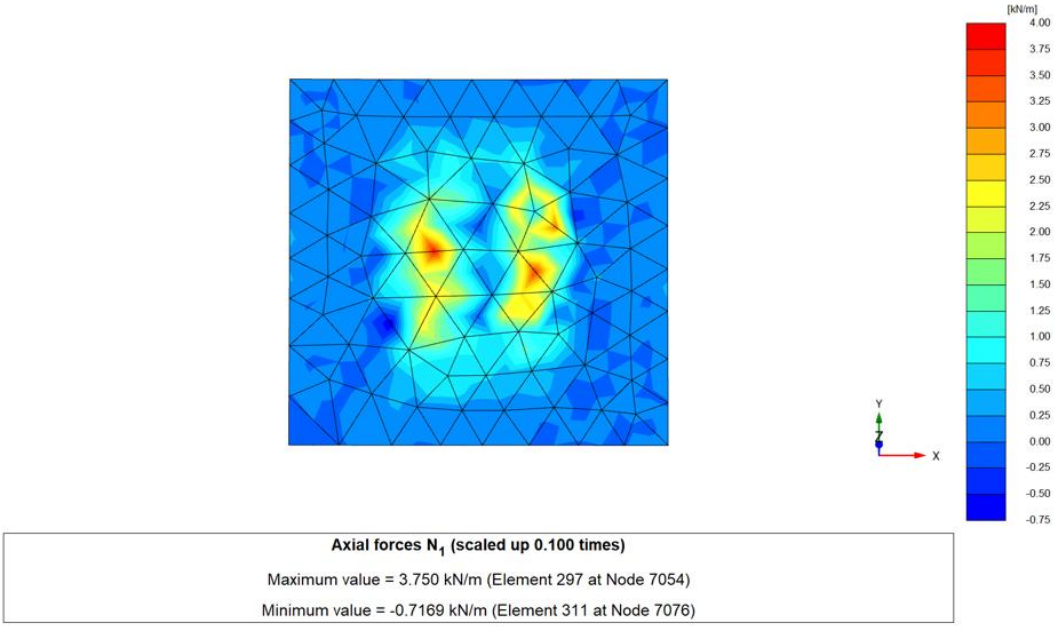

Figure 4.12 Axial force in second geogrid layer

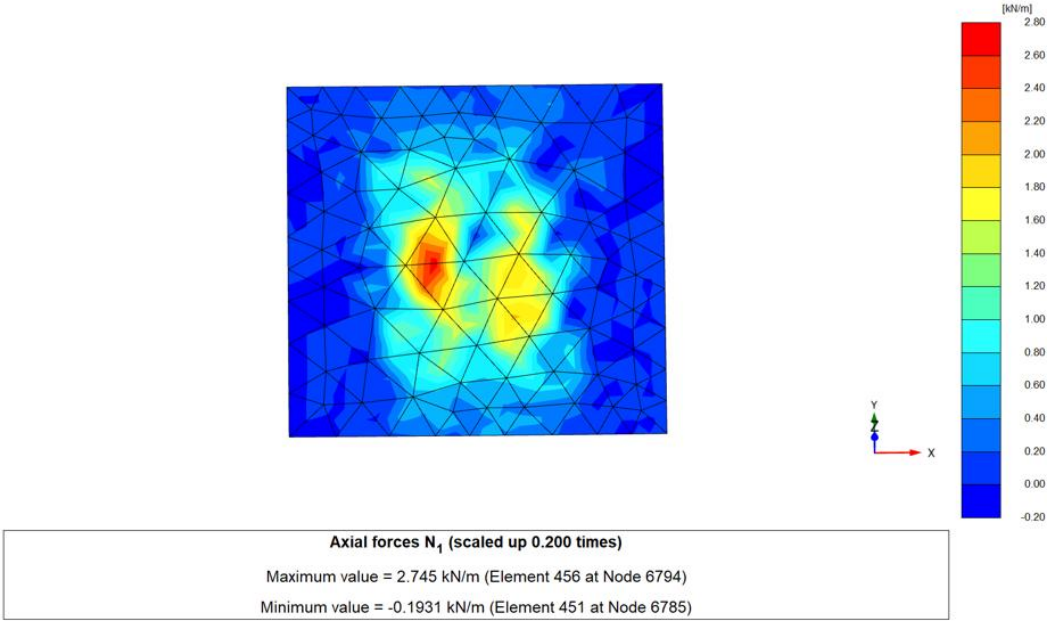

Figure 4.13 Axial force in third geogrid layer

This result implies that addition of reinforcement alone cannot significantly increases bearing capacity and reduces settlement. Thus, it can be concluded that effectiveness of reinforcement is governed by its position within stress influence zone rather than number of layers.

4.4 Effect of size of geogrid layer

To study the effect of size of geogrid, square shaped geogrid was considered and the length of geogrid was varied by adopting length of geogrid (L) as 1B, 2B, 3B, 4B and all other parameters was kept constant. Table 4.1 below shows the parameters considered in this study.

Table 4.1 Parameters considered for parametric study

Test series	Constant parameter	Variable parameter
	u/B=h/B=0.2, N=2, RD=50%, N=2	L/B=1,2,3,4

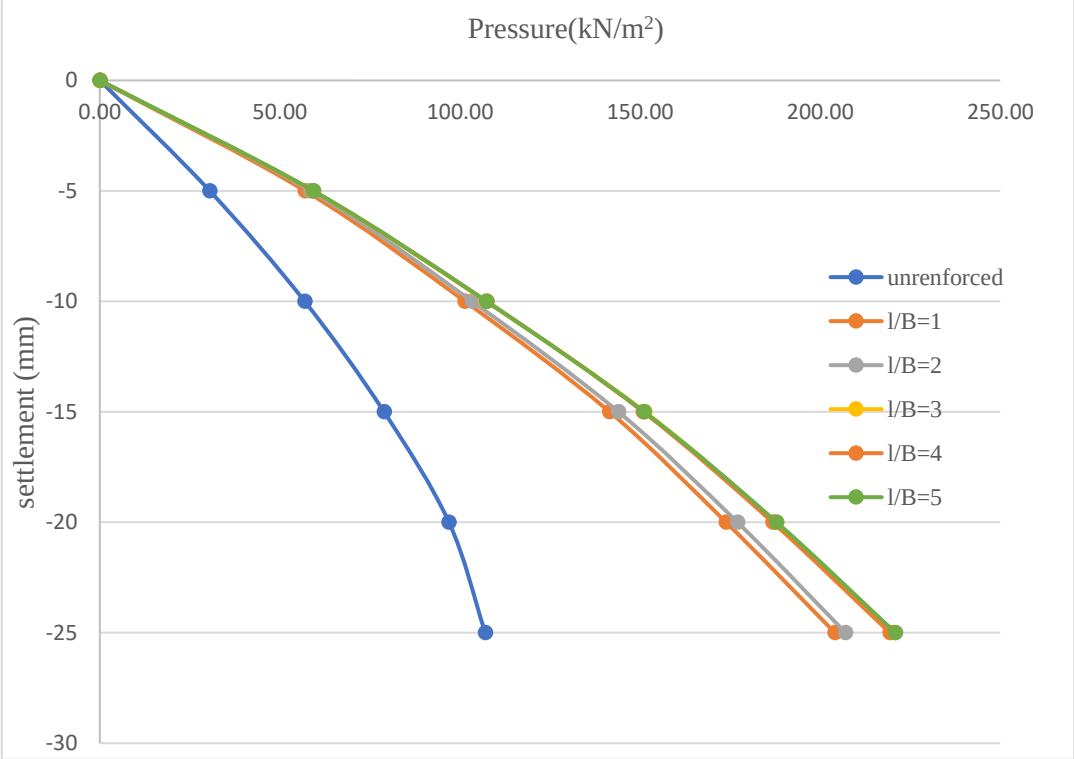

Figure 4.14 Load Vs settlement curve for different size of geogrid

Figure 4.14 illustrate load settlement response for various size of geogrid and it shows that bearing capacity increases as the length of geogrid increases up to l/B ratio of 3. Beyond this value further increment in length of geogrid do not increase the load carrying capacity and attain constant values. The magnitude of increase in BCR ratio is illustrated in figure 4.15 which shows that BCR increases more than twice compared to unreinforced footing at l/B ratio of 3. This is due to the fact that larger size of geogrid is effective for distributing load laterally. It was also

observed that settlement also decreases as the reinforcement size increases up to optimum size (l/B=3,4) and then attains a constant value.

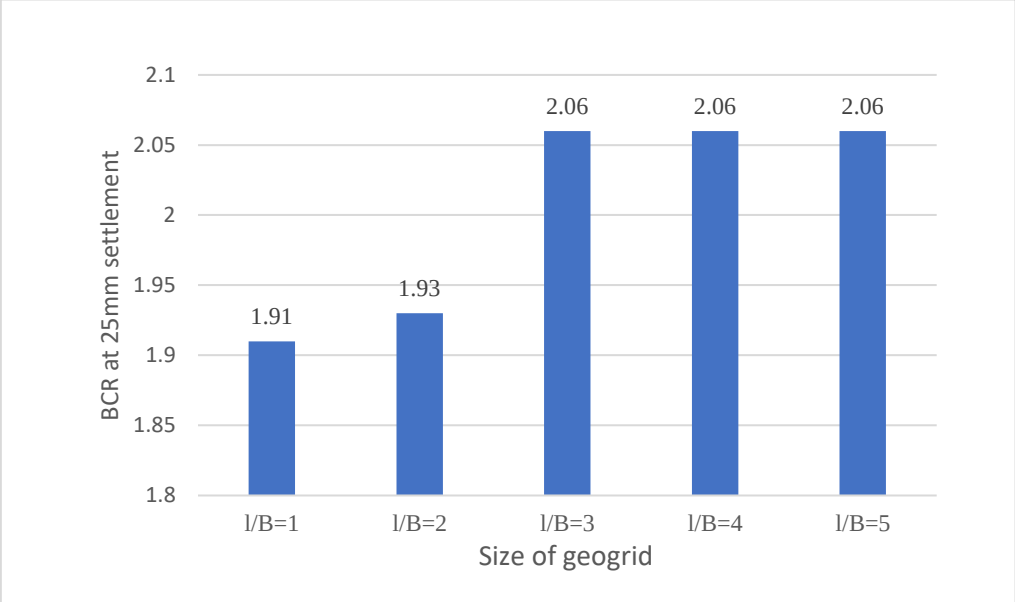

Figure 4.15 BCR for different size of geogrid

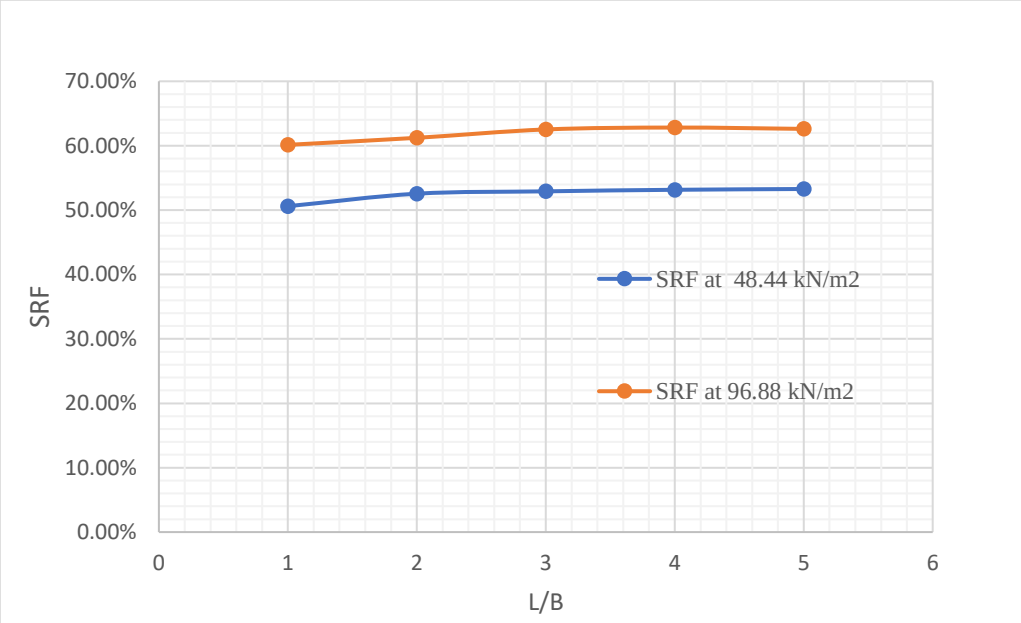

Figure 4.16 SRF for different size of geogrid layers

Thus, it can be concluded that larger size of geogrid increases bearing capacity and reduces settlement until it has reached its critical length and attains a constant value beyond further increment in length. At this length geogrid covers full lateral stress influence zone of footing and beyond l/B ratio of 3 and further increment

do not contribute and attains a constant value. In this study optimum size of geogrid is considered as l/B=3 for this study.

4.5 Effect of Relative density of sand fill

To study the effect of relative density of sand fill on geogrid reinforced footing, loose sand and medium sand of different relative density was considered in this study. The parameter considered for numerical analysis is as tabulated in Table 4.2.

Table 4.2: parameters Considered to study effect of relative density of sand

Test series	Constant parameter	Variable parameter
	u/B=h/B=0.2, N=2, l/B=3, N=2	RD 30% (loose sand) RD 50% (medium dense sand)

The load displacement curve becomes flatter as the relative density of sand fill increases indicating improvement in load carrying capacity. Figure 4.17 demonstrate that medium sand can resist higher load compared to loose sand at same settlement level. It is mainly attributed due to greater particle interlocking and higher frictional angle of soil which ultimately leads to increased shear strength of soil.

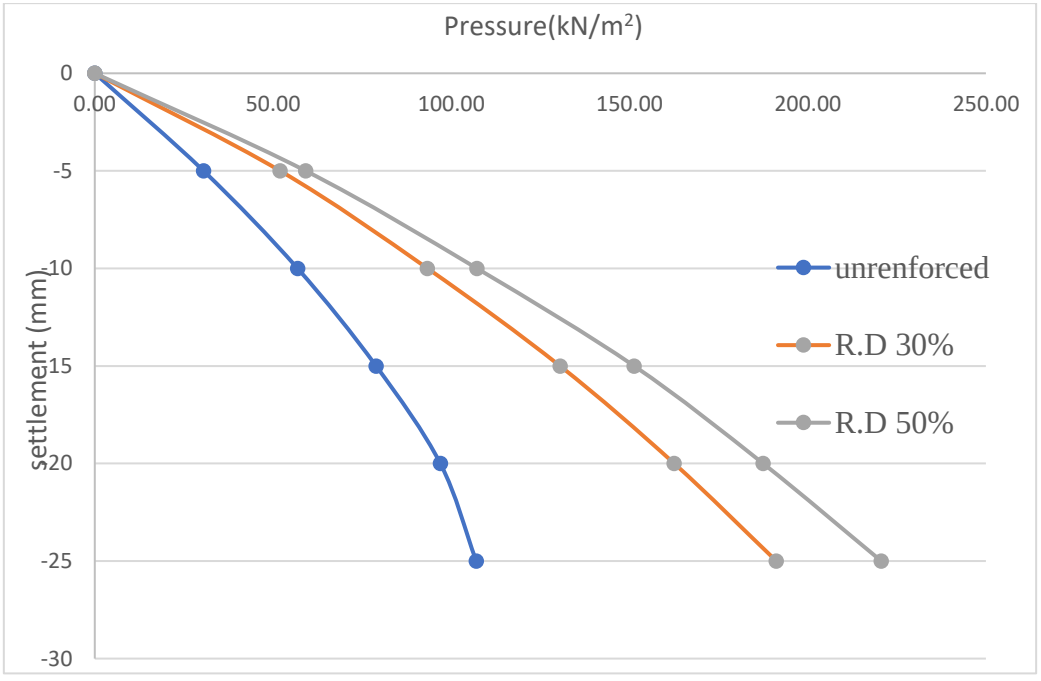

Figure 4.17 Load Vs settlement curve for relative density of sand

Figure 4.18 shows BCR improvement with dense sand is comparatively higher at all settlement level with maximum value of 2.06 than that of loose sand with BCR ratio of 1.79 at settlement level of 25mm.While maximum reduction in settlement was obtained with medium sand with SRF of 62.53% and 55.98% for medium dense and loose sand respectively at same bearing pressure of 96.88KN/m2 as in figure 4.19.Thus, it can be concluded that maximum improvement in BCR and SRF can be attained at higher relative density of sand fill due to enhanced interlocking and frictional resistance at higher relative density of sand which leads to better load transfer and efficient mobilization of geogrid tensile strength.

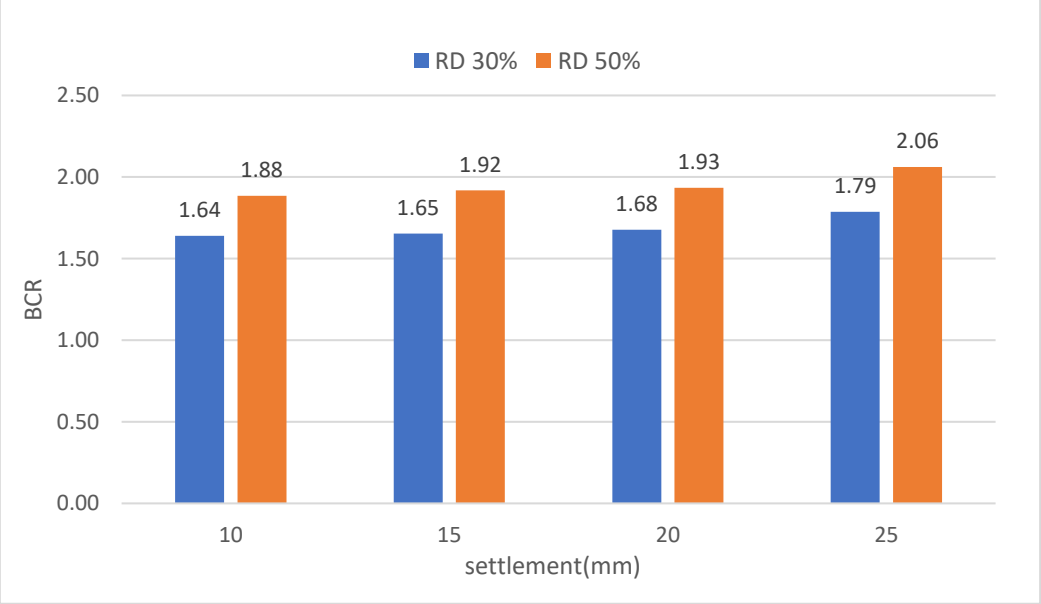

Figure 4.18 BCR for different relative density of sand

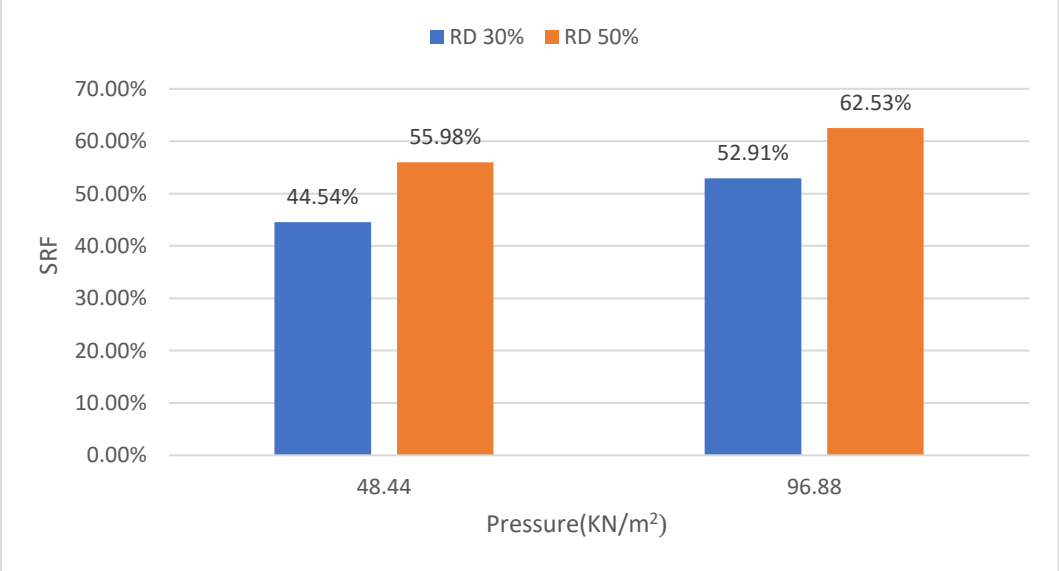

Figure 4.19 SRF for different relative density of sand

4.6 Effect of Thickness of sand Fill

Parametric analysis conducted to study the effect of thickness of sand fill in geogrid reinforced footing. Table shows the parameters considered for the study. Figure 4.20 shows pressure versus settlement curve obtained at different depth of sand fill which indicates that bearing capacity increase significantly with the increment in depth of sand fill. Figure 4.21 demonstrate the BCR at 25mm settlement with respect to different depth of sand fill which shows increase in improvement in BCR from 2.06 to 2.65 for D=0.75B to D=1.5B respectively. Thus, it can be concluded that partial replacement of weak soil layer with medium dense sand layer significantly improve bearing capacity. The improvement in settlement was also found to be significant with improvement as the depth of sand fill increases at both pressure level. At pressure of 96.88kN/m2 SRF ranges from 63% to 82% for depth of fill 0.75B and 1.5B respectively as illustrated in figure 4.22

Table 4.3: parameters for depth of sandfill

Test series	Constant parameter	Variable parameter
	u/B=h/B=0.2, N=2, l/B=3, RD=50% (medium dense sand)	D=0.75B, 1B ,1.25B ,1.5B

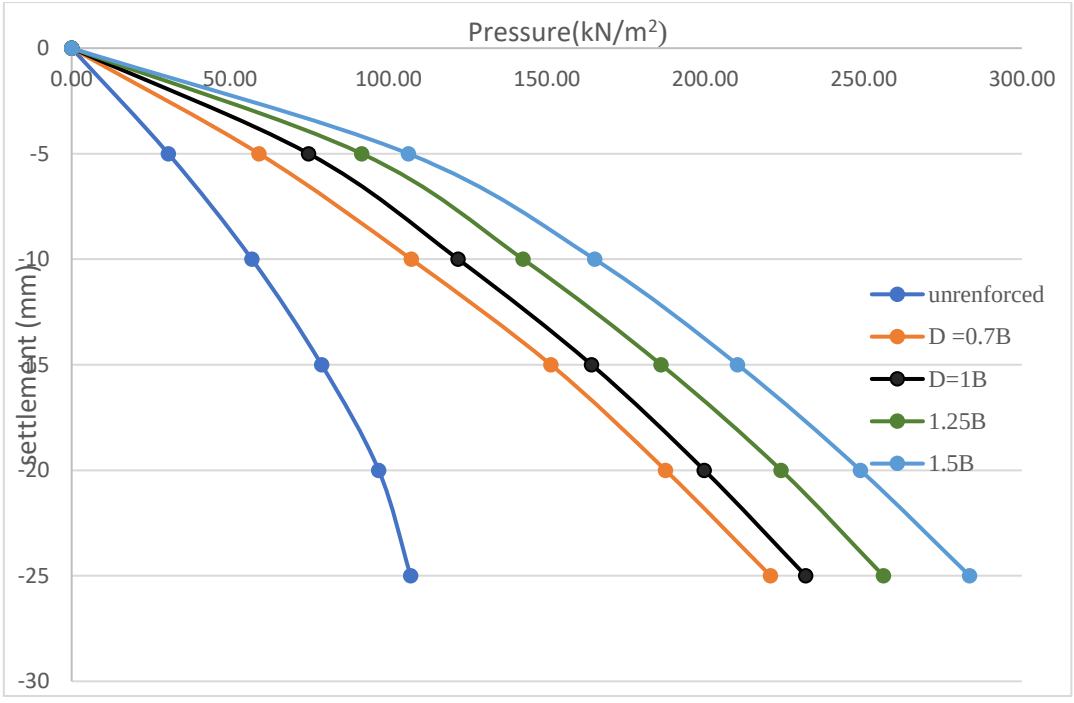

Figure 4.20 Load- settlement curve for variable depth of sand fill

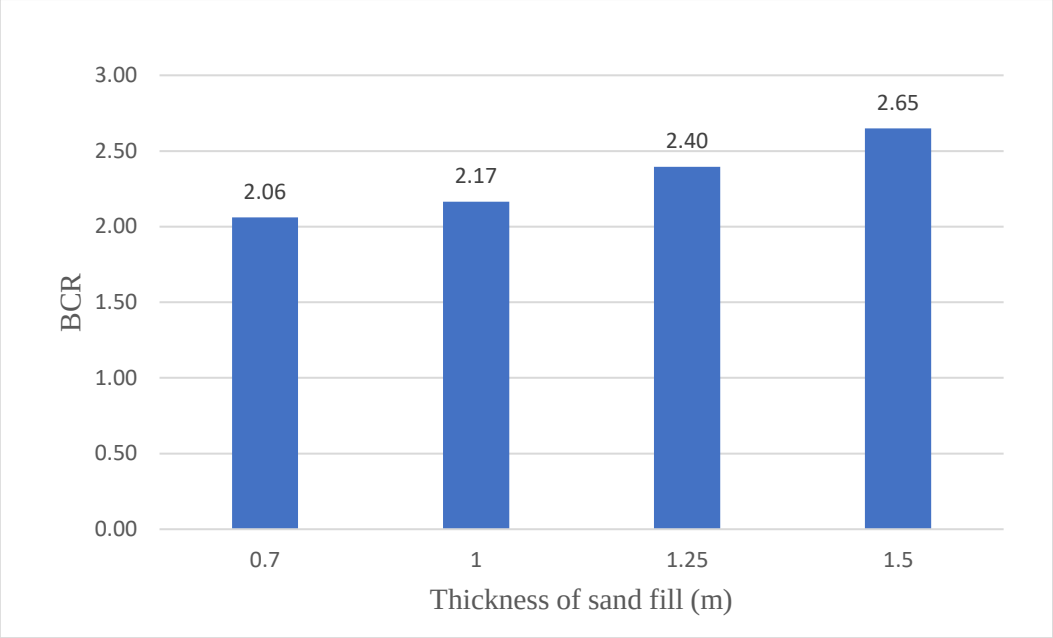

Figure 4.21 Bar graph showing BCR at variable depth of sand fill

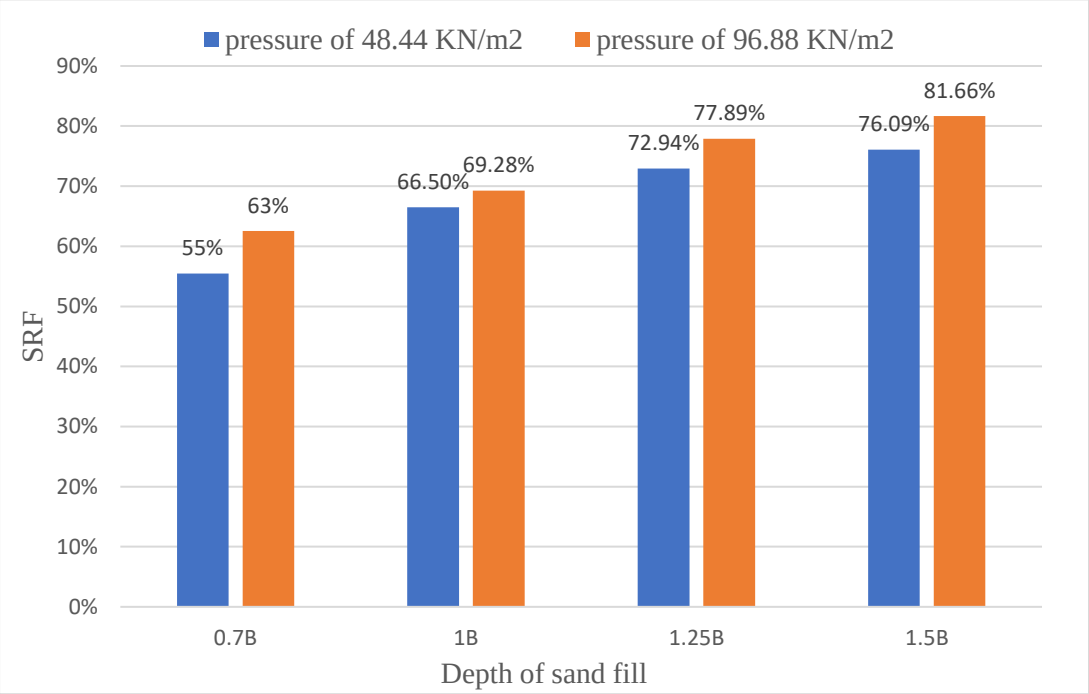

Figure 4.22 Bar graph showing SRF at variable depth of sand fill

This enhancement is due to the fact that sand has high friction angle and low compressibility than underlying silty soil and it acts as a strong and stiff layer, reducing the load intensity transmitted to soft soil subgrade. Increase in thickness of sand layer mostly confines stress bulb within sand layer resulting in increase in bearing capacity and reduction in settlement.

4.7 Effect of size of Footing

Numerical analysis was carried out to investigate the effect of footing size on bearing capacity of geogrid reinforced foundation. Various sizes of square footing were analyzed keeping all other parameter constant.

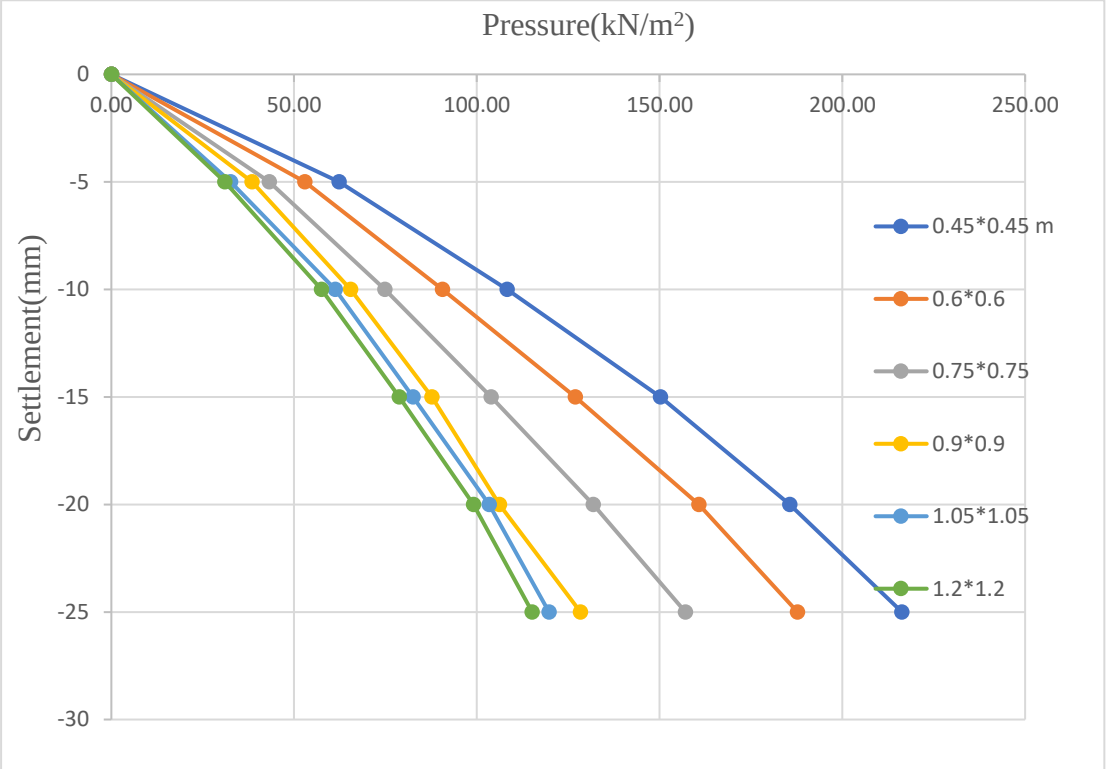

Figure 4.23 Load vs settlement curve for different size of foundation

It was observed that the load carrying capacity decreases as the size of footing increases as dissipated in figure 4.23 & 4.24. However, rate of decrease in bearing capacity decreases or becomes minimal after 0.9m*0.9m footing size. Similar trend of decreases in bearing capacity ratio were observed in numerical analysis of circular footing on sand (Useche-Infante et al., 2023).This is because the load required to achieve 25mm of settlement increases. However, the increase in load is not proportional to increment in area. Due to this reason bearing capacity and BCR ratio both decreases for larger footing size.

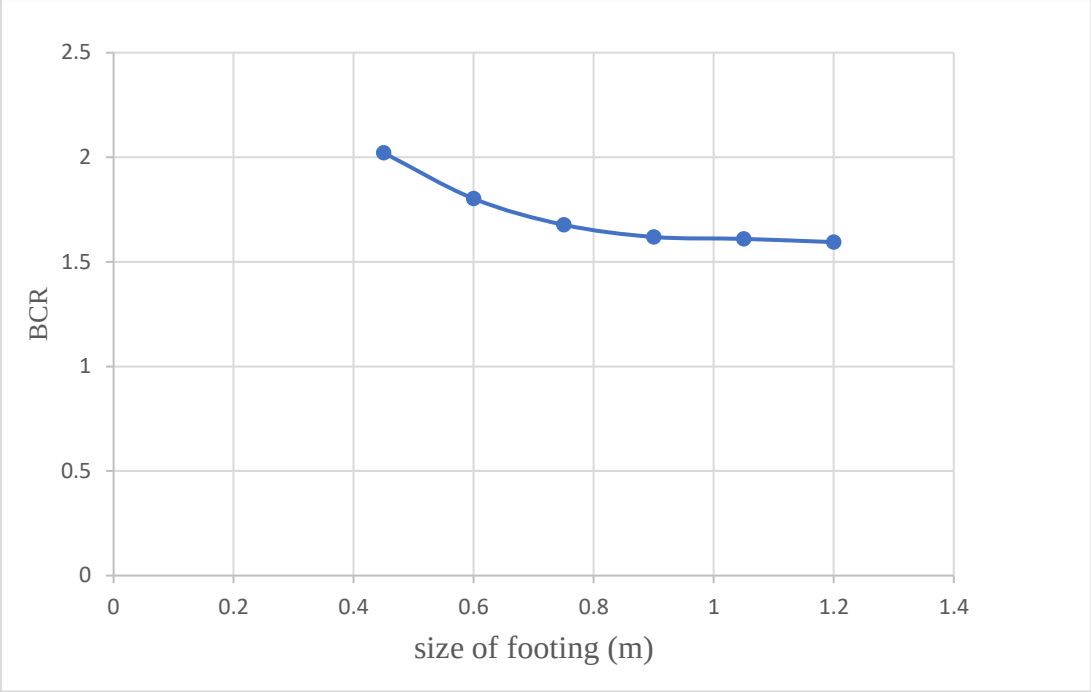

Figure 4.24 Variation of BCR with size of footing

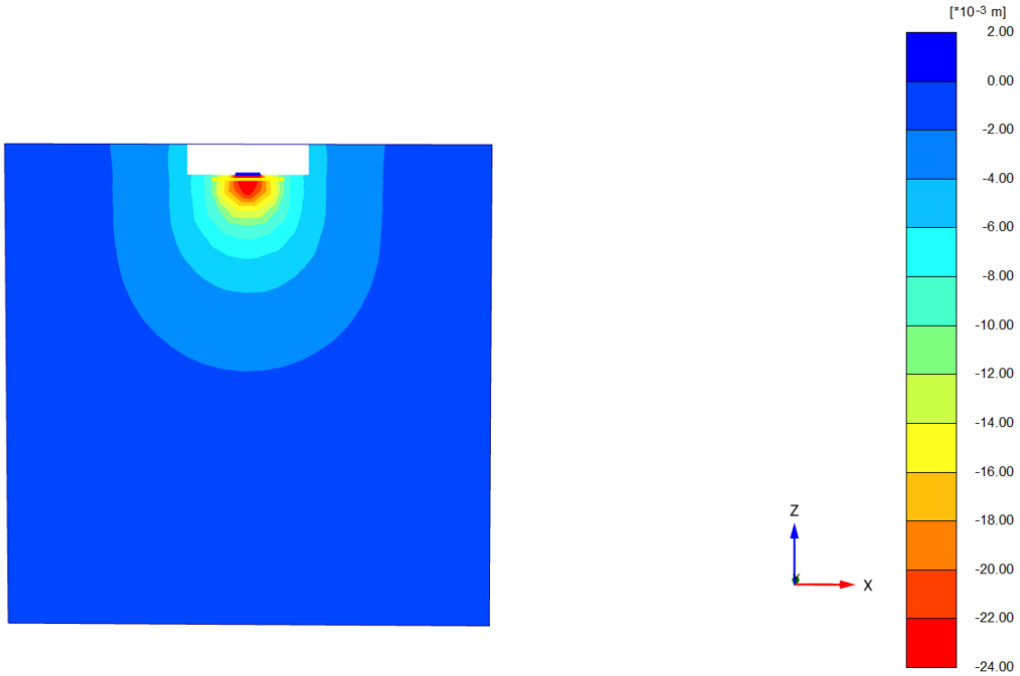

*Figure 4.25 Displacement contour for (1.2*1.2) m footing*

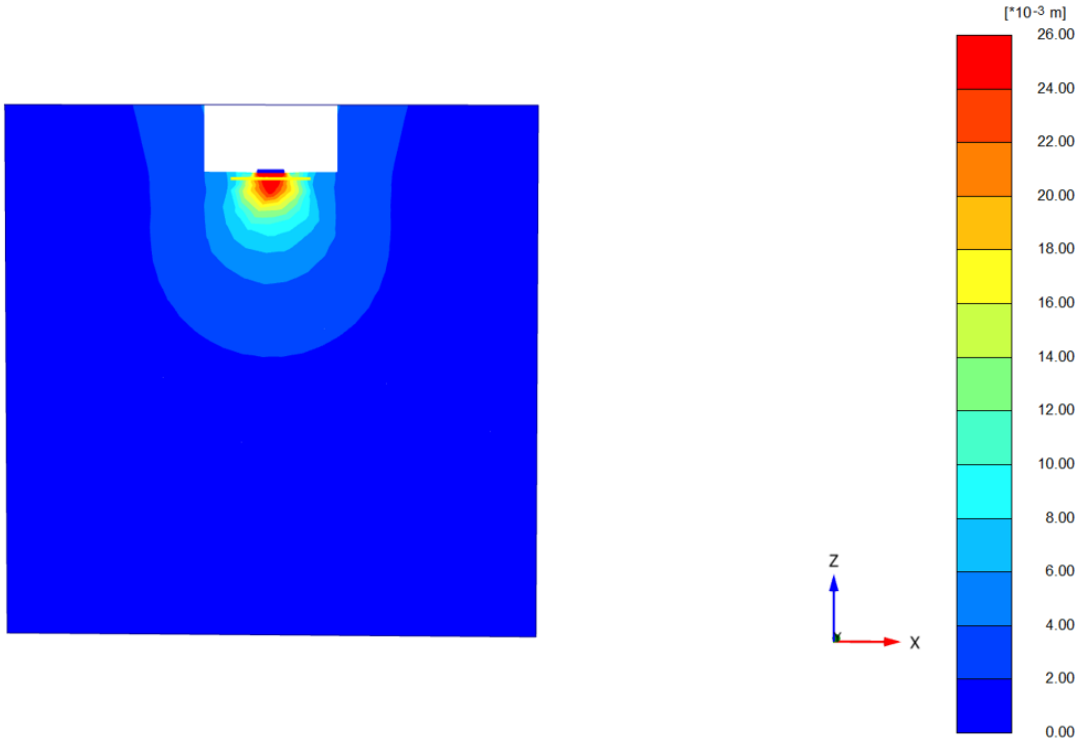

*Figure 4.26 Displacement contour for (0.6*0.6) m footing*

The displacement contours as shown in figure 4.25 &4.26 illustrate wider and deeper stress influence zone for (1.2*1.2) m footing whereas concentrated stress confined to shallow depth in case of small footing i.e. (0.6*0.6) m. This indicates greater amount of soil volume is mobilized in case of large footing.

Thus, it can be concluded that large footing mobilizes greater soil volume but the increase in load is not proportional to the area, causes decrease in bearing pressure at given settlement level and ultimately decrease in BCR.

4.8 Stiffness of Geogrid

Parametric study was conducted by varying the stiffness of geogrid and placing geogrid at optimum location. The bearing capacity increases with the increment of stiffness of geogrid with BCR of 1.98 to 2.05 at stiffness of 250 to 1250KN/m indicating moderate improvement. as shown in Fig 4.27. This show that stiffness cause slight improvement in bearing capacity. Similarly, settlement was reduced due to increment of stiffness of geogrid with improvement of 63% at 250kN/m and maximum of 64% at stiffness of 1250 kN/m. This minimal improvement might be due to low strain mobilization in reinforcement. These indicates that stiffness plays limited role for bearing capacity improvement and settlement reduction in case of soft silty soil condition.

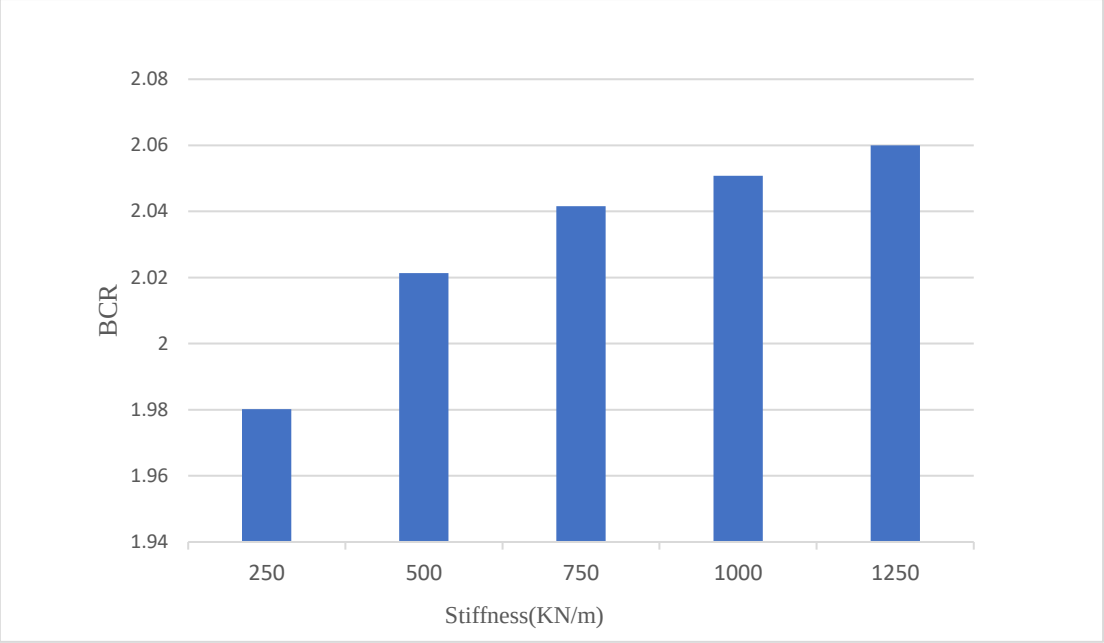

Figure 4.27:Variation of BCR with stiffness of geogrid

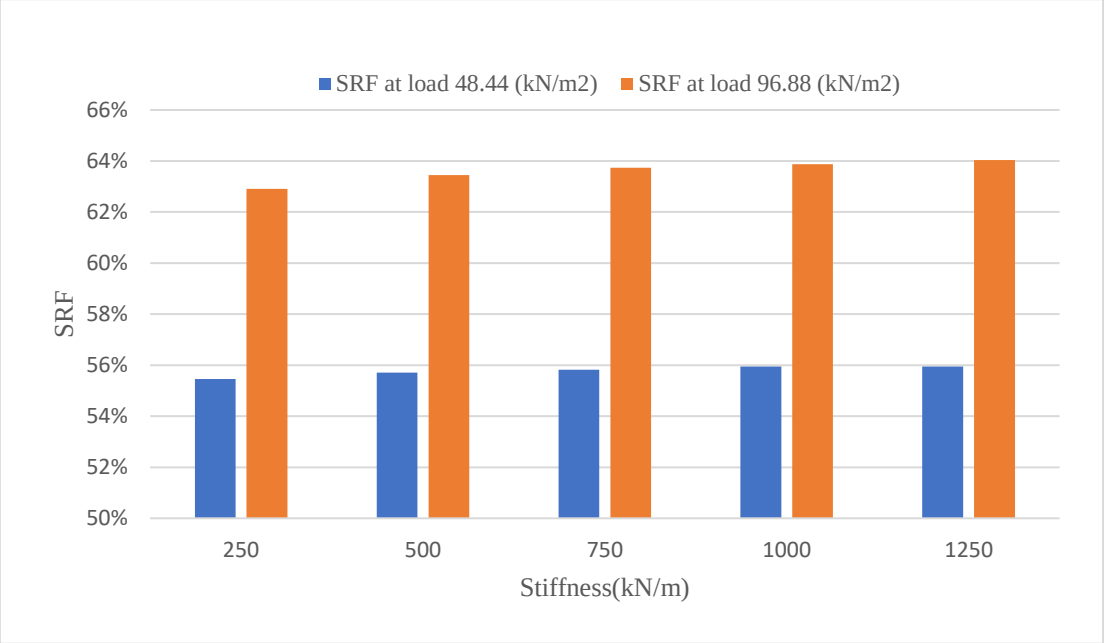

Figure 4.28: SRF at various stiffness of geogrid

4.9 Effectiveness of sand only, geogrid only and combined sand and geogrid

Finite element analysis was also conducted evaluate the effectiveness of sand cushion over soft subgrade layer, geogrid only and combined sand cushion reinforced with geogrid. Figure 4.29, 4.30 and 4.31 illustrate BCR, load settlement curve and SRF for sand, geogrid and combined sand and geogrid reinforcement. It was observed that load carrying capacity was increased with inclusion of sand cushion of thickness 0.7B below the footing, whereas geogrid layer was found to be less effective compared to sand fill for improving bearing capacity and compressibility of soil. The bearing capacity was significantly increased with maximum BCR ratio of 2.06 for combined sand and geogrid reinforcement followed by sand fill only and least improvement by use of geogrid layer only i.e., BCR ratio of 1.16 which is shown in figure 4.29. The SRF was quantified at pressure of 96.88 kN/m2 and the SRF value of 60% and 63% were attained for reinforcement using sand only and combined sand and geogrid respectively and the least improvement in settlement was achieved by using geogrid layer only.

Thus, it can be concluded that geogrid layer alone is not suitable for shallow foundation reinforcement in soft silty soil as frictional resistance between soil is very low due to which geogrid layer cannot confine soil mass and geogrid strength cannot be fully mobilized. While partial replacement of soft soil with sand layer was found to be effective but maximum benefit can be obtained when sand fill layers are reinforced with geogrid.

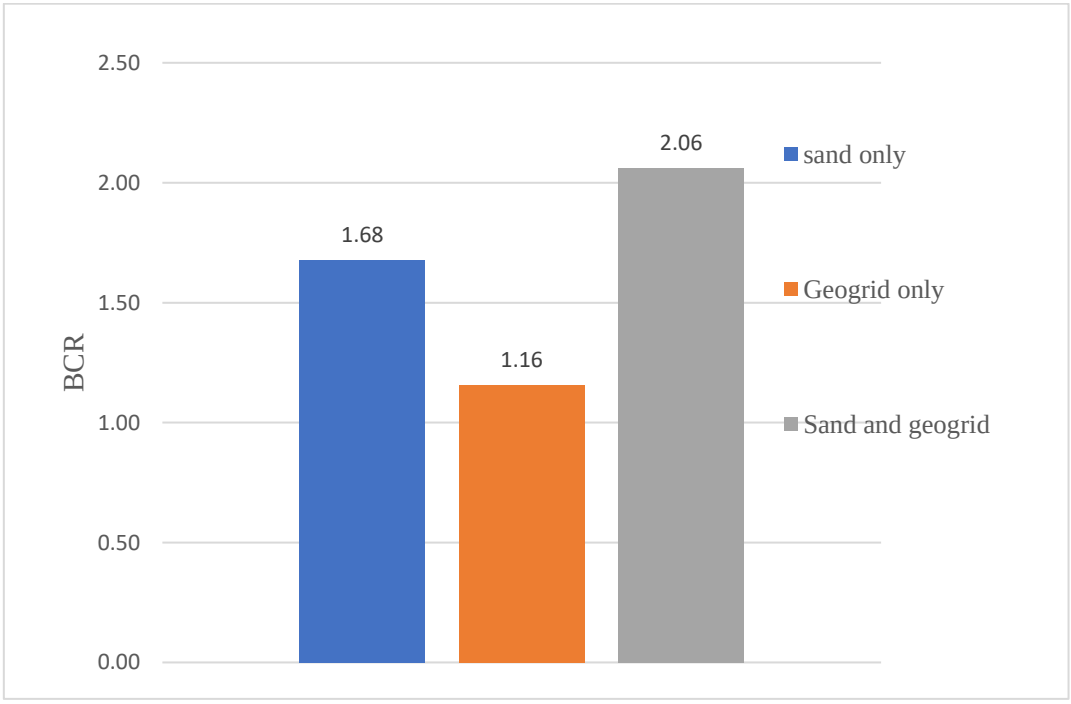

Figure 4.29: BCR for different method of foundation reinforcement.

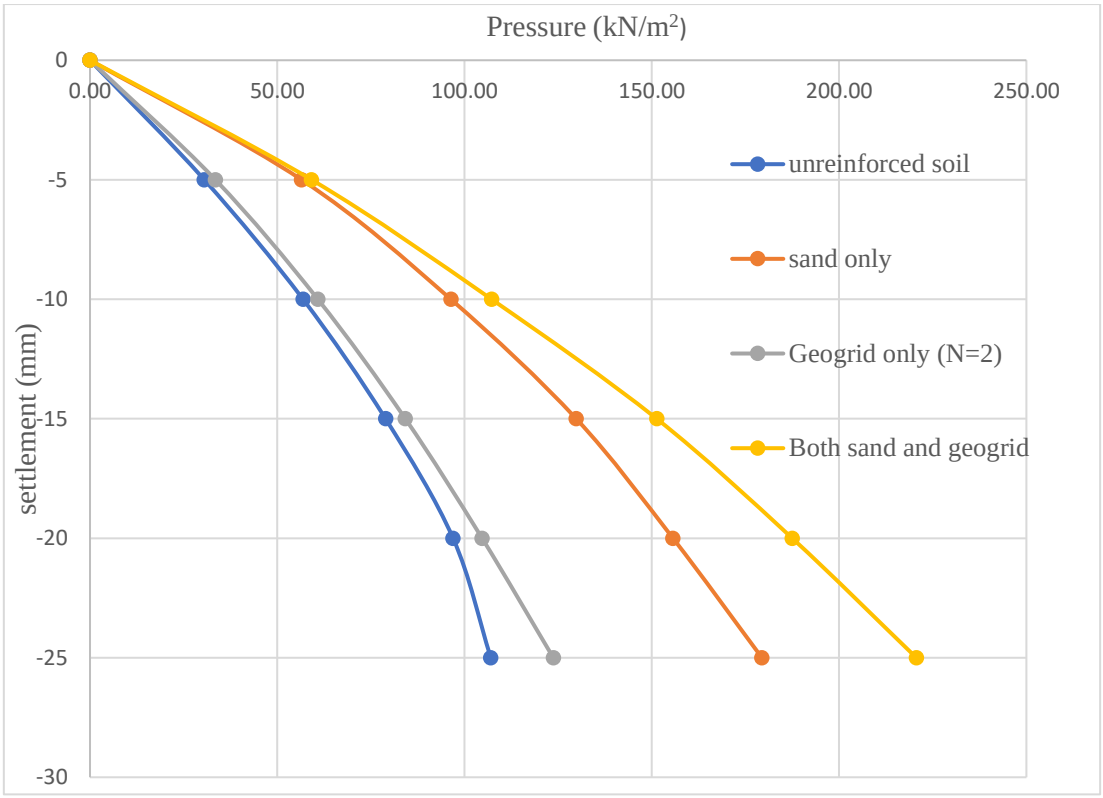

Figure 4.30: Load- settlement curve for different reinforcement method.

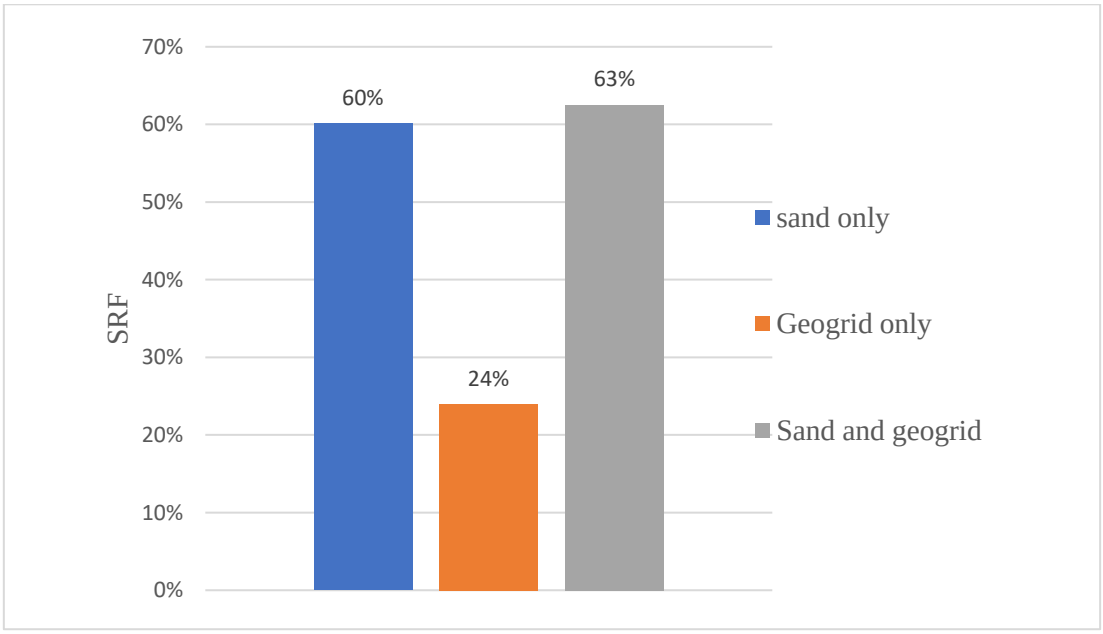

Figure 4.31: BCR for different method of foundation reinforcement.

5 CONCLUSION AND RECOMMENDATION

5.1 CONCLUSIONS

Three-dimensional analysis was conducted to assess the performance of a square footing resting on geogrid reinforced sand over low plastic silty soil. The key findings from this conclusion are listed below:

- The inclusion of geogrid reinforcement along with partial replacement of low plastic silty soil greatly improves bearing capacity and reduce settlement as compared to reinforcement with geogrid only or with sand replacement only. The inclusion of two layer of geogrid layer with sand fill of thickness 0.7B, BCR increases to 2.06 and SRF of 63% was attained in this study.
- BCR and SRF increases significantly with an increase in relative density of sand fill. For N=2, BCR of 1.79 and 2.06 and SRF increment from 55% to 62% at 30% and 50% relative density of sand fill respectively.
- The BCR and SRF significantly increases with the increase in thickness of replaced sand. BCR increases from 2.06 to 2.65 with an increment of about 60% and SRF increases by about 20% with increment in depth of sand fill from D=0.7B to D=1.5B.
- The optimum depth of placement of first geogrid layer and spacing between two geogrid layers was attained in between (0.2-0.3) B.
- It was observed that effectiveness of reinforcement is governed by its position within stress influence zone rather than number of layers.
- The BCR and SRF increases with increase in size of reinforcement up to l/B ratio of 3, with further increase in value it almost attains a constant value. Optimum size of geogrid can be considered as l/B =3.
- It was observed that bearing capacity for geogrid reinforced foundation decreases as the size of foundation increases at allowable settlement level.
- Increase in stiffness of geogrid slightly improves bearing capacity and settlement, however the rate of increase was found insignificant in this study.

5.2 RECOMMENDATION

This study is carried out within constraints of time and resources and could not address every aspect entirely. The recommendation for future work are outlined below:

- Numerical analysis can be conducted using advance hardening soil model.
- The research is limited to low plasticity silty soil. Further study can be conducted for high plasticity clay or expansive soil to better understand influence the geogrid reinforcement in variable weak or soft soil condition.
- It is recommended to perform laboratory or field model test and validate the result using numerical simulation to assure reliability and to obtain more accurate results.
- It is recommended to perform numerical analysis by inclusion of sand fill laterally to 3B to 5B to evaluate its influence on bearing capacity and settlement.
- The research is limited to static loading. This research can be done for cyclic or seismic loading condition.
- It is recommended to perform numerical analysis at ultimate level so that the effectiveness of geogrid at ultimate load can be analyzed.

REFERENCES

Abdolhosseinzadeh, A., Samui, P., Samaei, M., & Garousi, A. (2022). Numerical analysis of bearing capacity of circular footing reinforced with geogrid layers. *Arabian Journal of Geosciences*, *15*(8), 750. https://doi.org/10.1007/s12517-022-10030-8

Abu El-Soud, S., & Belal, A. M. (2019). Numerical modeling of rigid strip shallow foundations overlaying geosythetics-reinforced loose fine sand deposits. *Arabian Journal of Geosciences*, *12*(7), 254. https://doi.org/10.1007/s12517-019-4436-7

Alawaji, H. (2001). Settlement and bearing capacity of geogrid-reinforced sand over collapsible soil. *Geotextiles and Geomembranes*, *19*(2), 75–88. https://doi.org/10.1016/S0266-1144(01)00002-4

Albuja-Sánchez, J., Cóndor, L., Oñate, K., Ruiz, S., & Lal, D. (2023). Influence of geogrid arrangement on the bearing capacity of a granular soil on physical models and its comparison to theoretical equations. *SN Applied Sciences*, *5*(9), 250. https://doi.org/10.1007/s42452-023-05474-w

Arab, M. G., Omar, M., & Tahmaz, A. (2017). Numerical analysis of shallow foundations on geogrid reinforced soil. *MATEC Web of Conferences*, *120*, 06011. https://doi.org/10.1051/matecconf/201712006011

Benz, T., & Nordal, S. (Eds.). (2010). Validation of empirical formulas to derive model parameters for sands. In *Numerical Methods in Geotechnical Engineering* (0 ed., pp. 153–158). CRC Press. https://doi.org/10.1201/b10551-27

Bowles, J. E. (1996). *Foundation analysis and design* (5th ed). McGraw-Hill.

Chen, Q., & Abu-Farsakh, M. (2015). Ultimate bearing capacity analysis of strip footings on reinforced soil foundation. *Soils and Foundations*, *55*(1), 74–85. https://doi.org/10.1016/j.sandf.2014.12.006

Das, B. M. (2011). *Principles of foundation engineering* (7th ed). Cengage Learning.

Das, B. M. (2016). Use of geogrid in the construction of railroads. *Innovative Infrastructure Solutions*, *1*(1), 15. https://doi.org/10.1007/s41062-016-0017-8

Demir, A., Laman, M., Yildiz, A., & Ornek, M. (2013). Large scale field tests on geogrid-reinforced granular fill underlain by clay soil. *Geotextiles and Geomembranes*, *38*, 1–15. https://doi.org/10.1016/j.geotexmem.2012.05.007

Demir, A., Yildiz, A., Laman, M., & Ornek, M. (2014). Experimental and numerical analyses of circular footing on geogrid-reinforced granular fill underlain by soft clay. *Acta Geotechnica*, *9*(4), 711–723. https://doi.org/10.1007/s11440-013-0207-x

El Sawwaf, M. A. (2007). Behavior of strip footing on geogrid-reinforced sand over a soft clay slope. *Geotextiles and Geomembranes*, *25*(1), 50–60. https://doi.org/10.1016/j.geotexmem.2006.06.001

El-Attar, A. N., & El-Latief, A. A. (2024). Performance of square footing on geogrid reinforced soft clay. *Ain Shams Engineering Journal*, *15*(5), 102671. https://doi.org/10.1016/j.asej.2024.102671

Emirler, B., Tolun, M., & Yildiz, A. (2019). 3D Numerical Response of a Single Pile Under Uplift Loading Embedded in Sand. *Geotechnical and Geological Engineering*, *37*(5), 4351–4363. https://doi.org/10.1007/s10706-019-00913-1

Geotechnical Design Manual. (2010).

Guido, V. A., Chang, D. K., & Sweeney, M. A. (1986). Comparison of geogrid and geotextile reinforced earth slabs. *Canadian Geotechnical Journal*, *23*(4), 435–440. https://doi.org/10.1139/t86-073

Guo, X., Zhang, H., & Liu, L. (2020). Planar geosynthetic-reinforced soil foundations: A review. *SN Applied Sciences*, *2*(12), 2074. https://doi.org/10.1007/s42452-020-03930-5

K. C., N., & Raj Dahal, K. (2020). Investigation of Soil at Different Locations of the Kathmandu Valley of Nepal. *American Journal of Science, Engineering and Technology*, *5*(4), 167. https://doi.org/10.11648/j.ajset.20200504.16

Kolay, P. K., Kumar, S., & Tiwari, D. (2013). Improvement of Bearing Capacity of Shallow Foundation on Geogrid Reinforced Silty Clay and Sand. *Journal of Construction Engineering*, *2013*, 1–10. https://doi.org/10.1155/2013/293809

Latha, G. M., & Somwanshi, A. (2009). Bearing capacity of square footings on geosynthetic reinforced sand. *Geotextiles and Geomembranes*, *27*(4), 281–294. https://doi.org/10.1016/j.geotexmem.2009.02.001

Makkar, F. M. (2022). *Numerical Modelling of the Behaviour of 3D Geogrid Reinforced Soil Foundation*. *9*(6).

Makkar, F. M., Chandrakaran, S., & Sankar, N. (2017). Behaviour of Model Square Footing Resting on Sand Reinforced with Three-Dimensional Geogrid. *International Journal of Geosynthetics and Ground Engineering*, *3*(1), 3. https://doi.org/10.1007/s40891-016-0083-1

Obrzud, R. F., & Truty, A. (2018). THE HARDENING SOIL MODEL - A PRACTICAL GUIDEBOOK. *2018*.

Omar, M. T., Das, B. M., Puri, V. K., & Yen, S. C. (1993). Ultimate bearing capacity of shallow foundations on sand with geogrid reinforcement. *Canadian Geotechnical Journal*, *30*(3), 545–549. https://doi.org/10.1139/t93-046

-PLAXIS-3D-2024-1-3D-2-Reference-Manual. (n.d.).

Potts, D. M., & Zdravković, L. (2001). *Finite element analysis in geotechnical engineering. 2: Application*. Telford.

Sharma, R., Chen, Q., Abu-Farsakh, M., & Yoon, S. (2009). Analytical modeling of geogrid reinforced soil foundation. *Geotextiles and Geomembranes*, *27*(1), 63–72. https://doi.org/10.1016/j.geotexmem.2008.07.002

Shin, E. C., Das, B. M., Lee, E. S., & Atalar, C. (2002). Bearing capacity of strip foundation on geogrid-reinforced sand. *2002*.

Shukla, S. K. (Ed.). (2002). *Geosynthetics and their applications*. Thomas Telford.

Teku substation—Google Earth. (n.d.). Retrieved May 1, 2026, from https://earth.google.com/web/search/teku+substation/@27.69450596,85.30288438,1284.04592881a,1266.1046417d,35y,-62.99150854h,2.49497694t,0r/data=CjQiJgokCa7H3IRvtTtAEWLYDKuysDtAGecM-YB_VFVAIabMKIbYUlVAKgYIARIAGAFCAggBOgMKATBCAggASggI3rqn2QIQAA?utm_source=earth7&utm_campaign=vine&hl=en&authuser=0

Useche-Infante, D., Aiassa Martínez, G., Arrúa, P., & Eberhardt, M. (2023). Scale effect on the behavior of circular footing on geogrid-reinforced sand using numerical analysis. *Geomechanics and Geoengineering*, *18*(1), 34–47. https://doi.org/10.1080/17486025.2021.2007301

Yetimoglu, T., Wu, J. T. H., & Saglamer, A. (1994). Bearing Capacity of Rectangular Footings on Geogrid-Reinforced Sand. *Journal of Geotechnical Engineering*, *120*(12), 2083–2099. https://doi.org/10.1061/(ASCE)0733-9410(1994)120:12(2083)

ANNEX 1: BOREHOLE LOGS

BORE HOLE LOG

Date : Feb., 2021

Project: Soil Investigation Works for 132/11 kV Teku Substation Construction Site

Client: NEA Project Management Directorate (PMD), Kharipati, Bhaktapur

Location: Teku Substation, Kathmandu

Bore Hole No.: 3

Depth (m)	Thickness (m)	Classification	SOIL DESCRIPTION	Water Table (m)	SPT/DCP at (m)	No. of Blows per 15/10 cm Penetration 15/10	30/20	45/30	Total SPT/DCPT Value	Total SPT Value
					SPT 1.5	2	1	3	4	4
1.5	1.5	ML	Brownish soft, low plastic clayey silts with fine gravels							
				2.5	3.0	2	1	1	2	2
UD 4.0					4.5	2	1	2	3	3
	6.5	ML	Gray blackish soft, low plastic clayey silts with fine sands		6.0	3	2	2	4	4
8.0					7.5	3	2	3	5	5
					9.0	2	2	3	5	5
UD 11.0					10.5	2	3	3	6	6
	6.0	ML	Blackish medium, low plastic clayey silts with little fine sands		12.0	2	2	3	5	5
14.0					13.5	2	3	3	6	6
					15.0	2	3	3	6	6

ANNEX 2: LABORATORY TEST RESULT SUMMARY

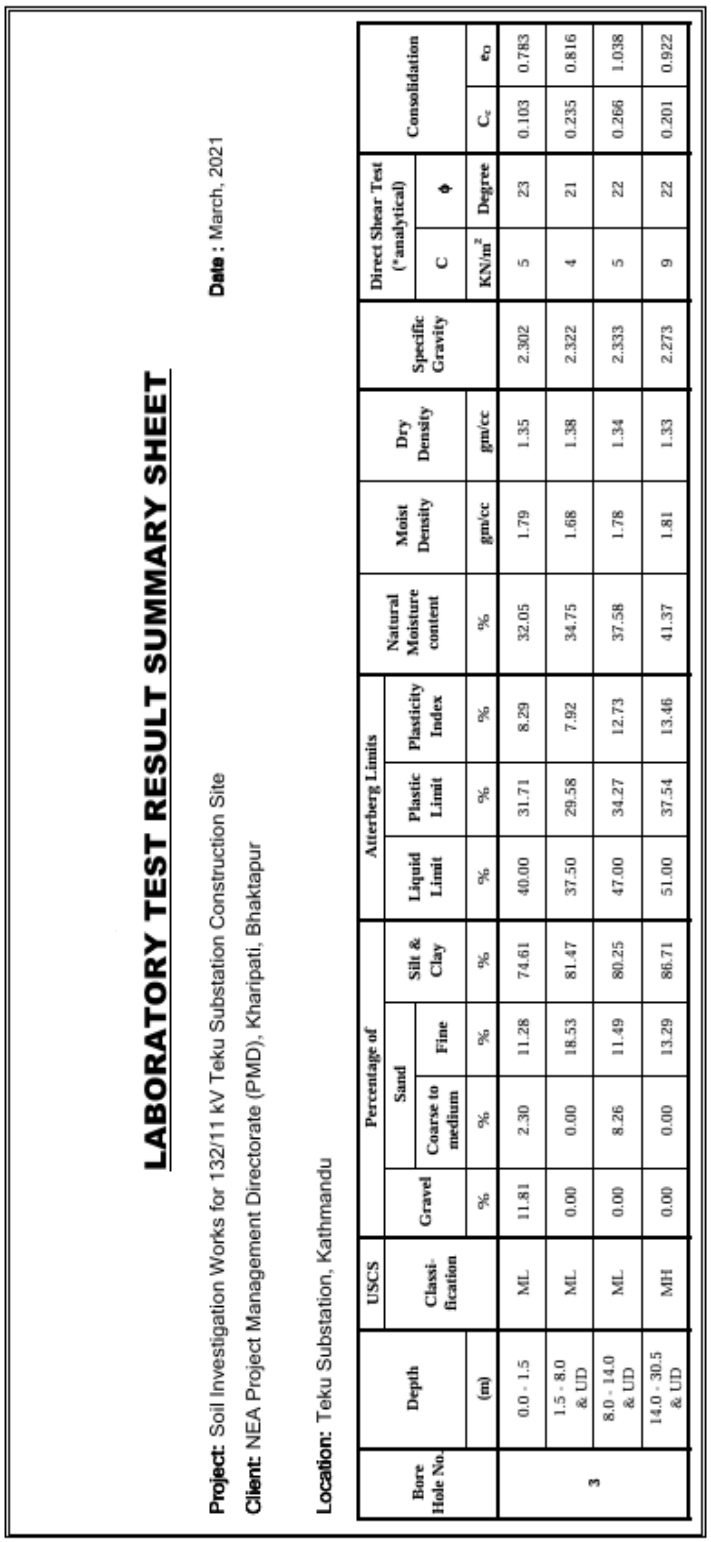

LABORATORY TEST RESULT SUMMARY SHEET

Project: Soil Investigation Works for 132/11 kV Teku Substation Construction Site

Date : March, 2021

Client: NEA Project Management Directorate (PMD), Kharipati, Bhaktapur

Location: Teku Substation, Kathmandu

Bore Hole No.	Depth	USCS Classi-fication	Percentage of				Atterberg Limits			Natural Moisture content	Moist Density	Dry Density	Specific Gravity	Direct Shear Test (*analytical)		Consolidation	
			Gravel	Sand		Silt & Clay	Liquid Limit	Plastic Limit	Plasticity Index					C	ϕ	C_c	e_0
	(m)		%	Coarse to medium %	Fine %	%	%	%	%	%	gm/cc	gm/cc		KN/m^2	Degree		
3	0.0 - 1.5	ML	11.81	2.30	11.28	74.61	40.00	31.71	8.29	32.05	1.79	1.35	2.302	5	23	0.103	0.783
	1.5 - 8.0 & UD	ML	0.00	0.00	18.53	81.47	37.50	29.58	7.92	34.75	1.68	1.38	2.322	4	21	0.235	0.816
	8.0 - 14.0 & UD	ML	0.00	8.26	11.49	80.25	47.00	34.27	12.73	37.58	1.78	1.34	2.333	5	22	0.266	1.038
	14.0 - 30.5 & UD	MH	0.00	0.00	13.29	86.71	51.00	37.54	13.46	41.37	1.81	1.33	2.273	9	22	0.201	0.922

ANNEX 3: PLATE LOAD TEST DATA

PLATE LOAD TEST SHEET

Date: 17th March, 2021

Project: Soil Investigation Works for 132/11 kV Changunarayan Substation Construction Site

Plate Size : 45 x 45 cm

Client: NEA Project Management Directorate (PMD), Kharipati, Bhaktapur

Settlement: 1 division = 0.01 mm

Area of Plate: 0.203 m^2

Location: Teku Substation, Kathmandu

Soil Type: Dark gray, low plastic clayey silts with fine sands with filling materials (ML)

Depth (m) : 1.5 - 2.0

S.No.	Load		Pressure	Deformation Measured Div																			
				Dial gauge	Dial gauge	Avg. Dial Gauge (1 & 2) Reading	Settlement	Dial gauge	Dial gauge	Avg. Dial Gauge (1 & 2) Reading	Settlement	Dial gauge	Dial gauge	Avg. Dial Gauge (1 & 2) Reading	Settlement	Dial gauge	Dial gauge	Avg. Dial Gauge (1 & 2) Reading	Settlement	Dial gauge	Dial gauge	Avg. Dial Gauge (1 & 2) Reading	Settlement
	(t)		(t/m²)	No. 1	No. 2			No. 1	No. 2			No. 1	No. 2			No. 1	No. 2			No. 1	No. 2		
				1 min	1 min	1 min	mm	2 min	2 min	2 min	mm	5 min	5 min	5 min	mm	10 min	10 min	10 min	mm	20 min	20 min	20 min	mm
1	0	0	0	0	0	0	0	0	0	0	0	0	0	0	0	0	0	0	0	0	0	0	0
2	1.0	4.94	600	590	595.00	5.95	612	605	608.50	6.09	635	640	637.50	6.38	650	655	652.50	6.53	660	670	665.00	6.65	
3	2.0	9.88	2500	2500	2500.00	25.00																	

ANNEX 4: PRESSURE VS. SETTLEMENT GRAPH

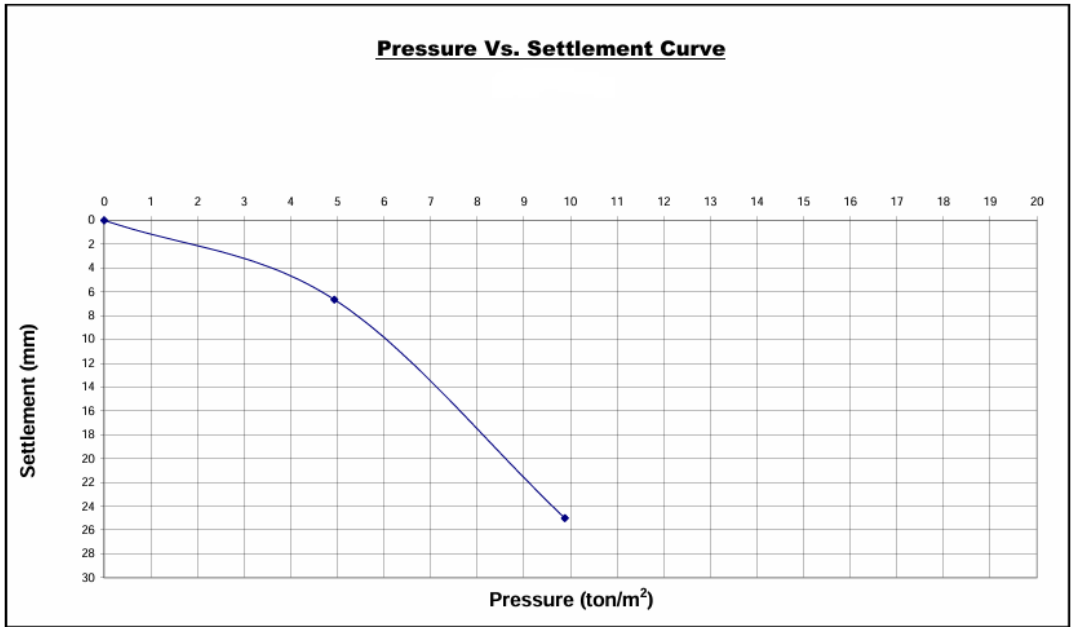

ANNEX 5: BCR CALCULATION SHEET

Test condition	Bearing pressure at different settlement level (KN/m2)					BCR at different settlement level				
settlement level	5 mm	10mm	15mm	20mm	25mm	5mm	10mm	15mm	20mm	25mm
Unreinforced soil	30.52	56.89	78.91	96.94	107.1					
u/B=0.1	60.10	105.63	146.12	179.01	208.74	1.97	1.86	1.85	1.85	1.95
u/B=0.2	62.32	108.25	150.27	185.58	216.30	2.04	1.90	1.90	1.91	2.02
u/B=0.3	59.46	106.91	149.58	185.28	217.83	1.95	1.88	1.90	1.91	2.03
u/B=0.4	57.04	102.02	138.77	170.07	197.88	1.87	1.79	1.76	1.75	1.85
u/B=0.5	58.02	102.77	144.15	175.65	205.43	1.90	1.81	1.83	1.81	1.92
h/B=0.1	60.40	108.35	152.35	189.19	222.12	1.98	1.90	1.93	1.95	2.07
h/B=0.2	59.16	107.21	151.31	187.51	220.64	1.94	1.88	1.92	1.93	2.06
h/B=0.3	59.36	106.17	149.93	184.10	215.85	1.94	1.87	1.90	1.90	2.02
h/B=0.4	59.75	105.53	148.99	184.10	215.85	1.96	1.85	1.89	1.90	2.02
h/B=0.5	53.48	95.70	132.35	163.26	190.12	1.75	1.68	1.68	1.68	1.78
N=1	62.32	108.25	150.27	185.58	216.30	2.04	1.90	1.90	1.91	2.02
N=2	59.16	107.21	151.31	187.51	220.64	1.94	1.88	1.92	1.93	2.06
N=3	59.75	106.62	151.06	187.41	220.44	1.96	1.87	1.91	1.93	2.06
l/B=1	57.04	101.38	141.53	173.88	204.10	1.87	1.78	1.79	1.79	1.91
l/B=2	58.42	103.36	144.00	177.04	207.06	1.91	1.82	1.82	1.83	1.93
l/B=3	59.16	107.21	151.31	187.51	220.64	1.94	1.88	1.92	1.93	2.06
l/B=4	59.21	107.46	150.86	186.81	219.36	1.94	1.89	1.91	1.93	2.05
l/B=5	59.36	107.36	151.16	187.95	220.89	1.94	1.89	1.92	1.94	2.06
D=0.75B	59.16	107.21	151.31	187.51	220.64	1.94	1.88	1.92	1.93	2.06
D=1B	74.86	122.02	164.15	199.75	231.75	2.45	2.14	2.08	2.06	2.16
D=1.25B	91.60	142.52	186.12	224.00	256.30	3.00	2.51	2.36	2.31	2.39
D=1.5B	106.32	165.14	210.27	249.04	283.51	3.48	2.90	2.66	2.57	2.65
RD=30%	52.00	93.33	130.52	162.57	191.21	1.70	1.64	1.65	1.68	1.79
RD=50%	59.16	107.21	151.31	187.51	220.64	1.94	1.88	1.92	1.93	2.06

Test condition	Bearing pressure at different settlement level (KN/m2)					BCR at different settlement level				
settlement level	5 mm	10mm	15mm	20mm	25mm	5mm	10mm	15mm	20mm	25mm
Unreinforced soil	30.52	56.89	78.91	96.94	107.1					
EA=250	61.93	106.81	147.56	182.07	211.90	2.03	1.88	1.87	1.88	1.98
EA=500	62.32	108.25	150.27	185.58	216.30	2.04	1.90	1.90	1.91	2.02
EA=750	62.52	108.94	151.70	187.51	218.47	2.05	1.91	1.92	1.93	2.04
EA=1000	62.67	109.33	152.40	188.44	219.46	2.05	1.92	1.93	1.94	2.05
EA=1250	62.77	109.63	152.89	189.09	220.44	2.06	1.93	1.94	1.95	2.06

Test condition	**Reinforced soil bearing pressure at different settlement level (KN/m2)**					**BCR at 25mm settlement level**				
	5mm	10mm	15mm	20 mm	25 mm					**BCR**
Footing size										
0.45*0.45	62.32	108.25	150.27	185.58	216.30	unrenforced soil with footing size(0.45*0.45)m @ 25mm			107	2.02
0.6*0.6	52.92	90.56	126.92	160.75	187.72	unrenforced soil with footing size(0.6*0.6)m @ 25mm settlement			104.2	1.80
0.75*0.75	43.18	74.79	103.89	131.84	157.05	unrenforced soil with footing size(0.75*0.75)m @ 25mm settlement			93.63	1.68
0.9*0.9	38.72	65.49	87.70	106.21	128.35	unrenforced soil with footing size(0.9*0.9)m @ 25mm settlement			79.27	1.62
1.05*1.05	32.65	61.22	74.87	103.40	119.73	unrenforced soil with footing size(1.05*1.05)m @ 25mm settlement			74.34	1.61
1.2*1.2	31.06	57.51	78.78	99.06	115.14	unrenforced soil with footing size(1.2*1.2)m @ 25mm settlement			72.22	1.59

ANNEX 6: SRF CALCULATION SHEET

Test condition	Settlement at different pressur		SRF at different pressure	
	48.44 kn/m2	96.88 kn/m2	5mm	25mm
Unreinforced soil	8.24	23.83		
u/B=0.1	3.79	9.02	54.00%	62.15%
u/B=0.2	3.65	8.71	55.70%	63.45%
u/B=0.3	3.84	8.92	53.40%	62.57%
u/B=0.4	4	9.58	51.46%	59.80%
u/B=0.5	3.96	9.36	51.94%	60.72%
h/B=0.1	3.79	8.82	54.00%	62.99%
h/B=0.2	3.88	8.93	52.91%	62.53%
h/B=0.3	3.86	8.96	53.16%	62.40%
h/B=0.4	3.82	8.99	53.64%	62.27%
h/B=0.5	4.43	10.19	46.24%	57.24%
N=1	3.65	8.71	55.70%	63.45%
N=2	3.88	8.93	52.91%	62.53%
N=3	3.85	8.93	53.28%	62.53%
l/B=1	4.07	9.5	50.61%	60.13%
l/B=2	3.91	9.24	52.55%	61.23%
l/B=3	3.88	8.93	52.91%	62.53%
l/B=4	3.86	8.86	53.16%	62.82%
l/B=5	3.85	8.91	53.28%	62.61%
D=0.75B	3.67	8.93	55.46%	62.53%
D=1B	2.76	7.32	66.50%	69.28%
D=1.25B	2.23	5.27	72.94%	77.89%
D=1.5B	1.97	4.37	76.09%	81.66%
RD=30%	4.57	10.49	44.54%	55.98%
RD=50%	3.88	8.93	52.91%	62.53%
EA=250	3.67	8.84	55.46%	62.90%
EA=500	3.65	8.71	55.70%	63.45%
EA=750	3.64	8.64	55.83%	63.74%
EA=1000	3.63	8.61	55.95%	63.87%
EA=1250	3.63	8.57	55.95%	64.04%